

Ion Formation Mechanisms in UV-MALDI

Richard Knochenmuss

Author's submitted version, subsequently published in *The Analyst*, vol. 131, pp. 966-986 (2006) DOI: 10.1039/B605646F,
URL:<http://www.rsc.org/publishing/journals/AN/article.asp?doi=b605646f>

Introduction

Modern mass spectrometry has undergone rapid change due to many factors, but not least thanks to development of two soft ionization methods, electrospray¹ and matrix-assisted laser desorption / ionization (MALDI).²⁻⁴ These have had considerable impact on many fields, particularly where large molecules need to be analyzed. Bioanalytics and synthetic polymers are examples of disparate applications which have profited enormously from these ionization techniques.

In spite of the very considerable effort expended in development and application of electrospray and MALDI, fundamental understanding of them has come relatively slowly. Both start from the condensed phase and progress to dilute gas or vacuum, making them dauntingly complex phenomena. In addition they might suffer from a certain interdisciplinary niche status- neither mainstream chemistry nor physics and hence more a target for applied rather than basic research.

Progress has nevertheless been made, and some agreement may be emerging on electrospray mechanisms.⁵⁻⁷ In contrast, MALDI development has been slowed by a lack of guiding mechanistic principles, leading to much empirical work. Consider the early efforts to identify good matrices, in which hundreds of compounds were briefly tried with a few analytes and given qualitative ratings.^{8, 9} Very few have entered common use, the handful of widely used matrices mostly were identified early on.⁹⁻¹⁴

This empirical approach to MALDI becomes less profitable as time goes on, but urgent analytical needs remain, as can be seen from the difficulties practitioners daily confront in absolute sensitivity, variable response factors, range of applicability and reproducibility. Without mechanistic understanding, the way forward is unclear. With it, we can either purposefully advance, or know when fundamental limits have been reached. Recent progress makes it appropriate to review the field now, in the hope of spurring new developments.

The goal is to quantitatively predict or interpret the observed mass spectrum as a function of all experimental variables. These are primarily: matrix choice, analyte physical and chemical properties, concentrations, preparation method, laser wavelength, spatial and temporal characteristics, local environment (such as ambient pressure or substrate temperature) and ion extraction method. This review is focussed on ionization mechanisms in MALDI using ultraviolet (UV) excitation, and so does not encompass all factors affecting a MALDI result. Infrared MALDI mechanisms are currently less well understood, but many aspects of UV models apply to infrared MALDI as well.

The matrices of interest here are generally solids, but the recently developed UV-absorbing ionic liquid matrices^{15, 16} probably function similarly since they are derivatives of conventional solid matrix molecules. New techniques involving interactions of matrix with metal substrates will be briefly discussed, but methods which (appear to) depend primarily on physical properties of the substrate will be excluded, such as desorption from laser-absorbing particles like those used by Tanaka¹⁷ or structured surfaces such as porous silicon¹⁸ or nanowires.¹⁹ These are probably dominated by thermal mechanisms due to the high peak temperatures reached during short pulse irradiation of strongly absorbing structures with poor thermal conductivity to the underlying bulk.²⁰

Ideas about MALDI ionization can be traced through the reviews and summary articles that have appeared over the years. Already in 1983 Hillenkamp was discussing characteristics of "true" laser desorption (and noted the variety of biomolecules under study).²¹ After the advent of modern MALDI in the mid 1980s,²⁻⁴ it was not long until significant reviews appeared.^{22, 23} A variety of possible mechanisms were under active consideration, Ehring, Karas and Hillenkamp²⁴ presented three excitation schemes with pathways leading to seven kinds of ions. Notably, the key intermediate step for all was highly excited matrix, foreshadowing some modern models. Liao and Allison²⁵ followed in 1995 with an extensive discussion of processes that could lead to protonated and sodiated adduct ions. This work was particularly progressive in that it recognized the central role of ion-molecule reactions in the MALDI desorption plume, and the relevance of the gas-phase thermodynamics of these reactions to observed mass spectra.

Karas, Bahr and Stahl-Zeng considered several aspects of matrix function in 1996, ranging from desorption to ionization and analyte fragmentation.²⁶ They emphasized proton transfer reactions of the matrix with analyte. The International Journal of Mass Spectrometry published a MALDI issue 1997 (vol. 169-170), but ionization was not extensively addressed. A review focussed on MALDI ionization mechanisms appeared in 1998.²⁰ In addition to an overview of the models then in use, the concept of distinct primary and secondary ion formation processes was explicitly introduced. The secondary reaction concept is reminiscent of the SIMS "selvege" idea.²⁷

In 2003 an issue of Chemical Reviews (vol. 103, nr. 2) was devoted to laser ablation of molecular substrates, and contains important contributions surveying several aspects of MALDI. Of particular importance are the microscopic view of the desorption/ablation event provided by the molecular dynamics work of the Zhigilei and Garrison groups,²⁸ the overview of MALDI desorption by Dreisewerd,²⁹ the synopsis of the recently developed cluster model by Karas and Krüger,³⁰ and the treatment of secondary mechanisms by Knochenmuss and Zenobi.³¹ The most recent collection of ionization-relevant papers will appear in an issue of the European Journal of Mass Spectrometry in 2006.

The two-Step Framework and Primary vs. Secondary Mechanisms

Current models of UV MALDI ionization have substantially converged in one important respect, that of the two-step framework: Initial (primary) ion formation or separation is the first step. Ion-molecule reactions in the desorption/ablation plume follow, giving rise to secondary ions which reach the detector. The various models for generation of primary ions are still somewhat divergent, but secondary reactions in some form are no longer controversial. The models of secondary processes are also converging. It is increasingly accepted that the plume is usually dense enough, long enough to apply conventional kinetics and thermodynamics. In other words, local thermal equilibrium is believed to be approached in the plume under typical MALDI conditions, in both UV and IR MALDI.

Both the two-step model and secondary models are fundamentally a consequence of the physical characteristics of the MALDI event, which will be briefly discussed next.

Physics of desorption/ablation

MALDI desorption/ablation has been extensively reviewed by Dreisewerd,²⁹ we note only the key observations here. The first role of the matrix is to absorb the laser energy and convert most of it to heat, causing the sample to disintegrate. Although this is an "energy-sudden" technique, the deposition time scale is not so dramatically short as in FAB or SIMS, for two reasons. First, the typical lasers used emit pulses of a few nanoseconds duration (e.g. N_2 , 337 nm, 3 ns or tripled Nd:YAG, 355 nm, 4-7 ns), although both shorter and longer pulses have been studied.³²⁻³⁶ This is slow compared to intramolecular motions. Second, and more important, the excited states of the matrix act as buffers, storing the laser energy and releasing it on a time scale similar to or longer than that of intra- and intermolecular relaxation. Excited state (generally S_1) lifetimes of free, gas phase, single matrix molecules are on the order of tens of nanoseconds, but are reduced to the order of 1 ns or less in the solid state by nonradiative pathways involving intermolecular interactions.³⁷⁻³⁹ The heat pulse from excited state decay can be no shorter than this, regardless of laser pulse duration, and so never reaches the femtosecond or low picosecond range which would lead to significant disequilibrium of different degrees of freedom.

The expansion of the material as it converts to a dilute gas is much slower, up to several microseconds. This difference in time scales is the origin of the two-step nature of MALDI. Processes which create separated ion pairs can only occur during or shortly after the laser pulse, because this requires concentration of energy. Later, the energy density is drastically reduced by conversion to heat and physical expansion, and the material begins to relax, both physically and chemically. Complete relaxation and thermal equilibrium is never attained because the expansion becomes so dilute that reactions effectively stop, and because ions may be extracted from the plume by applied fields. A schematic illustration of the time scales in MALDI is shown in Fig. 1.

Fig 1

As has been shown by simulations^{28, 40-44} and experiment,⁴⁵⁻⁴⁸ the disintegration event may be characterized as "desorption" or "ablation," depending on the laser fluence.

In the desorption regime, the solid to gas transition is smooth, at the top surface of the sample, and the emitted material contains little or no condensed particles, droplets or clusters. At higher, ablative, fluences the sample is sufficiently overheated that subsurface nucleation occurs, leading to "phase explosion," or turbulent, frothy, boiling. This ejects condensed material that can be captured on a cold plate and directly imaged,⁴⁶ or measured by aerodynamic sizing methods^{47, 48} In the MALDI context it is useful to differentiate between particles and clusters. The former are large aggregates of many molecules, and of macroscopic or mesoscopic size. Their properties are similar to those of bulk material. Clusters are small aggregates of a few molecules, which may have properties different from the bulk and from those of isolated molecules. Both particles and clusters are an important part of some models, and MALDI is often performed in the ablation regime. However, it should not be forgotten that aggregates which can be physically collected represent material which did not vaporize, so any ions within were not available for analysis. Examples of the desorption and ablation regimes are shown in snapshots of molecular dynamics simulations in Fig. 2.

Fig. 2

In addition to ablation due to phase explosion, another type of disintegration can occur under certain conditions. If the laser pulse is sufficiently short compared to thermal and mechanical relaxation of the irradiated volume, the material can experience stress confinement, leading to spallation of larger chunks or layers of material.⁴⁰ High amplitude expansion waves following the laser-induced compressive wave can exceed the cohesive strength of the material well below the surface. This is not believed to be common for typical MALDI experiments, since it requires either short pulses (tens of picoseconds) or atypically high pulse energies. The spallation chunks also will not have sufficient internal energy to fully vaporize, since they are mechanically rather than thermally ejected from relatively cold layers of the sample.

The temperatures at which typical matrices have high vapor pressures and hence high desorption fluxes are moderate. Values of a few 100° C have been suggested⁴⁹ For a MALDI event, the threshold surface energy density and temperature appear to be independent of excitation characteristics such as wavelength or pulse width, for a given matrix.⁵⁰ MALDI is thus correlated with the vapor pressure achieved during the laser pulse. Consistent with this, the minimal laser fluence required is strongly correlated with the initial sample temperature.^{51, 52} The heat of matrix sublimation, however, is not correlated with MALDI efficiency,⁵³ even though it represents the energy required to remove a given amount of material from the surface.

Reports vary regarding peak sample temperatures in UV MALDI, partly because it is dependent on laser pulse energy. Measurements of physical properties in the plume give values around 500 K^{54, 55} Recent efforts using "thermometer" molecules with well-

defined unimolecular decay kinetics^{56, 57} allow inference of higher values, around 1000 K, but interpretation of the fragmentation yield data in terms of temperatures is not without complication. One report of infrared emission measurements suggests similarly high temperatures,⁵⁸ but IR emissivities of matrix materials are not known, especially at elevated temperatures, so uncertainty remains in the results. Theoretical models are consistent with the experimental ranges, giving values between 600 and 1200 K, for typical MALDI fluences.^{59, 60} The material initially cools rapidly due to the phase transition then more slowly as the gas expands. The simulations also show that the gas does not have a uniform temperature, but rather a gradient, due to the depth-dependent energy deposition by the laser.

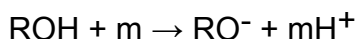
The gas pulse, or plume, undergoes a dramatic density reduction during the MALDI event: from solid density to high vacuum (or 1 atm in some instruments). This has been compared to adiabatic supersonic expansions used for creation and isolation of very cold molecules and clusters.^{60, 61} This analogy is appropriate, but it must be recalled that a polyatomic gas does not cool strongly. Adiabatic cooling depends on the heat capacity ratio C_p/C_v , which is largest for monatomic gases, and nearly 1 for molecules such as MALDI matrices.⁶² For this reason molecular beam experiments are always carried out with a large excess of rare gas as carrier of the molecules of interest. Decomposition of some matrices to low molecular weight neutral fragments (such as CO_2) may aid in expansion cooling, as well as accelerate the plume. These fragments are a central part of the pneumatic assistance model discussed below.

The plume has been modeled using hydrodynamic equations⁶³⁻⁶⁶ and as a pre-accelerated adiabatic expansion.⁶⁰ The time scale for density reduction to collision free conditions is, as noted above, orders of magnitude larger than that of the laser pulse. These models do not directly account for the mixed gas/cluster/particle nature of the plume in the ablation regime, but are still useful as a first approximation. They also do not reflect changes in plume development as the complex crater shape develops and deepens during a single laser shot, or over the course of several shots in the same place.^{67, 68} The mixed-phase aspect of ablation arises naturally in molecular dynamics, with the disadvantage is that it is not possible to perform simulations over the full temporal and spatial extent corresponding to most experiments, for computational reasons. Nevertheless, molecular dynamics has provided impressive insight into numerous aspects of the phase transition aspect of MALDI.^{28, 43, 69-73}

Ion Energetics, Matrix and the Plume

When discussing MALDI ion generation, it is important to recall the limiting energetics of the process. Breaking a C-H or O-H bond to yield R^- and H^+ requires about 14 eV or 1350 kJ/mol. Compare, for example the value reported for the hydroxyl proton of phenol: 14.65 eV.⁷⁴ This would be a 4.2-photon event with a 355 nm laser, and hence not a very probable direct process. Even "preformed" ions such as salts of matrix or analyte must still be separated into individual ions, although this is less endothermic than for covalent bonds.

Of course the ions are not formed in vacuo but in the condensed matrix, early in the expansion. Matrix molecules have significant proton affinities, so mH^+ will be formed in the above example (m =matrix), and the energetics are more reasonable: around 5 eV or 480 kJ/mol for:



Such reactions will be discussed further below, but this illustrates an important point: MALDI ionization probably always relies on assistance from the matrix in a variety of ways.

But the role of the matrix does not end with facilitation of initial charge separation. It is still necessary to fully isolate the charges so they can be transferred to the mass analyzer. After initial partial separation, an ion pair may still have a few eV of Coulomb attraction, and will recombine in the absence of further influences. Again the matrix supplies the necessary assistance, in the form of collisions. Since plume temperatures are moderately high, so are thermal collision energies. This is apparent from the axial plume velocities, mean values are a few 100 m/s, but the distributions extend past 1000 m/s,^{61, 75-80} although analytes tend to be somewhat slower than the fastest matrix ions^{78, 80, 81} and the distributions can be somewhat non-thermal (see below). Individual collisions can impart over 1 eV, so final ion separation by multiple collisions in the early plume is usefully frequent. This has been shown in detail in molecular dynamics simulations.⁵⁹

Primary Ionization Mechanisms

Generation of the first ions in MALDI remains the most controversial aspect of the method. Of the two main modern approaches for UV-MALDI, one argues that excited matrix is intimately and crucially involved, another views the matrix as mainly the desorption/ablation vehicle. We begin with the latter.

The Cluster Model

This model was proposed and largely developed by the Karas group, the "cluster" label refers to aggregates of any size, not just small clusters as defined here. It began as the "lucky survivors" model.⁸² The ions were taken to be largely preformed in the solid matrix, and undergo extensive neutralization in the plume, often by electrons in the case of positive ions. Hence the moniker- it seems meant to emphasize an incomplete, stochastic recombination process which leaves us some useful ions at the end. It has since been developed further with somewhat less emphasis on electrons.³⁰ Some of the key processes in this and other cluster models are sketched in Fig. 3.

Fig. 3

The focus on preformed ions arises from the observation that analytes are often charged in the preparation solution, with the subsequent hypothesis that they retain this charge in the matrix solid, much as in crystallization of an ionic material like salts. The main direct

evidence for this was the preparation of MALDI samples of pH sensor dyes, from solutions of different pH.⁸³ The solid samples tended to retain the color of the original solution, indicating that the dye molecules had the same de/protonation state as in solution.

This is a very interesting result, but the fate of the counterions cannot be inferred from the color. The same issue arises for any analytes that are charged in solution, either naturally or "charge tagged" by derivitization.⁸⁴⁻⁹³ All analytes which are ionic in solution are very probably closely associated with the appropriate counterions in the solid sample prior to desorption. This is also true of added or opportunistic salts which lead to cation complexes in the mass spectrum. Consistent with this are indications of a gas-phase pickup process,⁹⁴⁻⁹⁷ although "backside" desorption would seem to suggest otherwise.⁹⁸ Many matrices are highly ionized in polar solvents, but solids are molecular in nature, so the matrix generally does not contribute preformed ions.⁹⁹

In the cluster model some counterion separation is a result of photoionization and loss of the resultant electrons from the sample, which thereby acquires a net positive charge. This undoubtedly occurs, but not to a large extent. Electron capture cross sections have subsequently been measured for MALDI matrix materials,^{100, 101} allowing demonstration that only a thin, few nm, top layer loses electrons, in the remaining material they are captured to form matrix anions (leading to further secondary products).¹⁰² There is also a limit to positive surface charging, given by the electric field at which photoelectrons have insufficient energy to escape, and fall back to the surface.¹⁰²

The major charge separation is instead suggested to occur mechanically during ablation. Rapid disintegration of the solid matrix may sometimes lead to an excess of positive or negative charge on aggregates. These must then either evaporate by loss of neutral matrix to free the analyte ions, or the ions must be ejected. In this picture, the ion yield under desorption conditions, where vaporization is smooth, should be negligible. This is not consistent with experiment, MALDI ions can be observed at fluences where aggregates are not found.

Charge in a cluster or particle may internally migrate (via proton, cation or electron transfer), to yield the most favorable ions, this falls into the category of secondary reactions, as does any intra-aggregate neutralization. Electrons originally figured prominently in neutralization, but more recent developments of the model have also recognized the importance of matrix anions.³⁰

Among the earliest studies invoking clusters in MALDI ionization was work by Kinsel et. al,^{103, 104} where insulin ion flight time distributions were investigated. It was concluded that these resulted either from late release of ions entrained in the dense plume, or downstream secondary reactions. Krutchinsky and Chait used MS/MS to show that the "chemical noise" in MALDI spectra is often composed of charged clusters with a high matrix content.¹⁰⁵

Recently, the Tabet group has also investigated late ions from a cluster viewpoint. Using a variable repulsive potential prior to ion extraction in a time-of-flight spectrometer, they selected ions with a large effective initial m/z ratio, much larger than that of the ion observed later after inversion of the field.^{106, 107} Using 2 common matrices and various analytes, they interpreted the peak shapes as evidence for massive precursors of up to 50000 Da, containing many matrix molecules. The detected ions were proposed to result from complete evaporation of the aggregates, possibly assisted by collisions during extraction of ions through the neutral gas by external fields.

Cluster/particle vaporization ("desolvation") has been considered in detail by this group.¹⁰⁸ They find evidence for both "hard" and "soft" pathways. The soft path is characterized by loss of neutral matrix, so the net charge does not decrease during desolvation. The observable associated with this is a high yield of multiply charged analytes. In contrast, charged matrix is ejected in "hard" desolvation, so only low analyte charge states result. Further, these two pathways should have different kinetics, depending on the exothermicity of matrix-analyte proton transfer and the characteristics of the associated transition states. This means the charge state of a given analyte can be modulated by matrix choice, which is somewhat consistent with experimental experience.

The entrainment/late release and cluster/particle interpretations of the data would not appear to be entirely compatible. Current evidence indicates that delayed ion formation is not limited to conditions of very large cluster formation. In addition, simulations show extensive ion entrainment, but when clusters form, they usually do not contain sufficient internal energy to fully evaporate. These results are more consistent with entrainment, but further study is clearly needed.

The Photoexcitation/Pooling Model

Direct two- or multi-photon ionization of matrix or matrix-analyte complexes does not generally appear to be a major contributor to UV-MALDI, as will be discussed below. Instead, a combined model of excitation energy migration in the matrix, followed by concentration of this energy in "pooling" events has been developed.

Pooling was one of several energy concentration possibilities imagined in early work.²⁴ It is a phenomenon in which the electronic excitation energy of two nearby molecules is redistributed. Consider neighboring molecules which are both individually raised to the first excited singlet state (S_1) by photoexcitation. If these excited states have significant interaction due to wavefunction overlap, the coupled system may distribute the total energy in various ways. In addition to the nominal 1 quantum / molecule ($S_1 : S_1$), an isoenergetic state formally has 2 quanta on one molecule and none on the other ($S_n : S_0$). When this has nonnegligible probability, high energy processes become possible via pooling.

Pooling would be of limited importance for MALDI if it were necessary to rely on excited pairs randomly created by the laser. For these to be sufficiently numerous, rather high

intensities are needed.³⁹ However, if excitations can move in the matrix, this limitation is lifted. Mobile excitations can be treated as pseudo-particles and are known as excitons.^{109, 110} This form of energy transport depends on similar wavefunction overlap of packed chromophores as does pooling, but here the overlap is between one excited molecule (S_1) and one in the ground state (S_0).

Exciton migration and pooling have long been known in solid-state aromatics,^{111, 112} but have been studied and demonstrated in only one MALDI matrix, 2,5 dihydroxybenzoic acid (DHB). The onset of pooling is reflected in fluorescence quenching, as recognized early by Ehring & Sundqvist.^{113, 114} The topic was taken up again by Lüdemann, et al.,³⁸ but the fluence range covered did not allow unequivocal characterization of the pooling. Later studies covered a larger range, demonstrating that quenching by pooling stopped at low fluence, and also used time-resolved emission and trapping by dopants to show that S_1 excitons are mobile and undergo pooling annihilation reactions in DHB.³⁹ The time per hop is about 50 psec, so excitons can migrate a substantial distance within the 0.5-1.5 nsec excited state lifetime. It was also shown that analytes with excited states below those of the matrix can be efficient exciton traps, reducing MALDI efficiency, another indicator of the involvement of matrix excitations in MALDI ionization.

Two photons from N_2 or tripled Nd:YAG lasers are not sufficient to ionize free DHB molecules or many other matrices,^{115, 116} so a $S_1 + S_1$ pooling event is not expected to generate ions. Instead this leads to a higher excited state, S_n (which may also be reached by photoexcitation). Pooling of an S_1 with an S_n excitation is energetically sufficient for ionization. This sequential pooling model has been expressed in the form of coupled differential equations, and used for quantitative MALDI predictions.⁶⁰ The intra- and intermolecular processes involved are sketched in Fig. 4. The second pooling step was characterized by a time-delayed 2-pulse experiment,¹¹⁷ in which a delay of 2-3 ns between subthreshold pulses yielded the maximum matrix ion yield.

Fig 4

A key aspect of this model is the interaction between excited state processes, including ionization, and the physical expansion. Since exciton hopping, pooling, quenching and recombination are all second order, their rates are strongly dependent on the intermolecular collision rates. These in turn depend on the local temperatures and pressures in the plume. The expansion in turn is determined by the rate of energy conversion from excited electronic states (including ions) to heat, and the resulting pressure gradient. The plume can then be described as a molecular beam emitted from an aperture defined by the laser spot. It is a pre-accelerated expansion because thermal expansion causes significant forward motion prior to the phase change.

Fig. 5

Given local near-equilibrium, the molecular-level processes can be described by rate equations, which are integrated numerically. An example result is shown in Fig. 5. Clusters and particles are relevant in this model only to the extent that this fraction of ejected material is taken to create no free ions, and is deducted from the final result. A potential weakness of this approach is the transition from dense solid to an expanding plume. Since this happens within nanoseconds, non-equilibrium conditions may briefly exist. These are outside the range of validity of the expansion equations.

To evaluate this difficulty and to better investigate the physical/chemical interactions in MALDI, the pooling model of ionization was added to the molecular dynamics method of Zhigilei and Garrison to form a complete molecular-level MALDI model.⁵⁹ This allows better insight into coupling of ionization with the expansion in desorption, ablation and spallation regimes, all of which can coexist in different layers of the sample. As expected, the role of excited states in storing energy, and thereby moderating the phase transition is particularly important.

Because the photoexcitation/pooling model is quantitative, it can be compared in detail with a variety of experimental data, if the matrix is sufficiently characterized. Currently the only such matrix is DHB, but many other matrices exhibit very similar phenomena, so more general applicability seems possible or even probable. Some of the data it reproduces or explains for DHB are:

The most important correctly predicted quantity is the ion yield. The ratio of ejected ions to neutrals in a MALDI event is in the range of 10^{-4} to 10^{-3} , depending on fluence, corresponding well with experiment.^{45, 55, 118-120}

The fact that MALDI is laser fluence (J/cm^2), not irradiance (W/cm^2) dependent, within the range of typical laser pulse lengths^{32, 35, 121-123} (although activation of analytes may be more sensitive to the rate of energy deposition.¹²⁴) This is a general feature of many matrices. For DHB it clearly stems from the excited state energy storage effect noted above. However, irradiance independence is only valid to a certain point. When the time scale for energy deposition becomes much longer than the excited state lifetime, MALDI efficiency decreases for a given fluence, as shown by time-delayed 2 pulse experiments.¹¹⁷

A characteristic of MALDI which is quickly apparent to users of all matrices is the fluence "threshold." MALDI ion generation has a high-order (approximately 6-th power) empirical dependence on fluence.^{55, 120} This means that ions may be observed even at very low fluences, given sufficient detection sensitivity. However, strong ion signal is only observed when significant material is ejected, leading to a perceived threshold effect. In most instruments it appears as if no signal is generated up to some laser intensity, after which it is easily observed. Although ion yield has a higher than linear dependence on fluence via the density of excited states, the model predicts that many ions are formed at relatively low fluence, but most are simply not emitted because little material vaporizes. In the absence of ablation, only the few that escape in desorption events at the sample

surface can be detected. Because the apparent threshold is not dominated by ion formation, positive and negative ions have the same fluence threshold, as found experimentally.¹²⁵ Similarly, the ion yield as a function of elevated initial sample temperature is largely a matter of desorption/ablation efficiency.⁵² This indicates that the plume-ionization interaction is largely correct in the model, since the expansion characteristics change considerably over the temperature range studied. However, the steepness of the fluence dependence of ion yield is not well predicted by the model, and is in the range of 2-3.

Also connected with material ablation is the positive correlation of the solid state matrix absorption spectrum with MALDI efficiency. A higher absorption coefficient gives a lower threshold,^{2, 126} so a relatively small change in wavelength can disproportionately affect efficiency, although the nature of the ions observed remains the same (i.e. the ionization processes do not change). Higher absorption coefficients lead to higher energy density in the upper sample layers. This has two beneficial effects. First, since ionization is a nonlinear function of excited state density, many more ions are created in the top layers. Second, greater heating leads to larger material ejection and ion release from those layers. The 337 and 355 nm fluences where the thresholds appear are correctly predicted for DHB.

The MALDI yield is dependent on the degree of laser focusing, in a nonlinear manner.^{55, 121, 127} This is also a physical rather than chemical effect, and is readily understood from the expanding jet picture of the plume. The key parameter in adiabatic expansions is the x/d ratio, where x is the distance downstream, and d is the orifice diameter. In MALDI this "orifice" is the laser spot. This means bimolecular processes "freeze-out" faster in a plume emitted from a small spot due to lateral expansion. Yield per ejected volume is higher for a small spot as a result of less extensive recombination in the plume, but since the ablated volume increases quadratically with increasing spot diameter, total yield per laser shot is nevertheless larger from bigger spots.

Other possible contributors to MALDI primary ionization

While the above two primary ionization models currently appear to be the most widely discussed, this does not mean that other mechanisms do not contribute to MALDI, they probably do. We next briefly discuss some of these.

- Direct multi-photon ionization of matrix or matrix-analyte complexes

The ionization potentials (IPs) of matrix molecules lie in the 3-photon region for typical MALDI lasers, compare that of DHB, at 8.054 eV.¹¹⁵ Most matrices are aromatics with similarly sized conjugated pi-systems, and so have similar IPs. IPs can also be calculated with reasonable accuracy by *ab initio* methods (within about 0.2 eV).^{116, 128-131} See Table 1 for some selected values. Three photon processes are normally very inefficient at MALDI-like irradiances, but could become significant if picosecond or femtosecond lasers are used.

However, it is not free molecules which are ionized in MALDI, but matrix and analyte in a

matrix environment. Collective effects such as charge delocalization nearly always reduce IPs compared to isolated molecules. The IPs of matrix clusters have received limited study, but only insignificant reductions (a few tenths of eV) were found in DHB clusters.¹³² While the "IP" (work function) of bulk matrices remains unknown, it appears that even large reductions would not be important in practice, because a severe decrease in photoionization efficiency was observed for clusters at low energy.¹³²

Potentially much more important for MALDI are IP reductions due to matrix-analyte interactions. Especially if electron or proton accepting groups are present, intermolecular charge transfer can lead to facilitated photoionization of the coupled system, via the matrix chromophore. The Kinsel group has performed several studies showing this effect in clusters.¹³³⁻¹³⁶ Not only were strongly reduced IPs found for DHB-proline complexes (down to 7 eV),¹³³ post-ionization fragmentation leading to protonated analytes was observed in matrix-biomolecule clusters.^{135, 136}

Ab initio calculations have reproduced both IP reductions and ion-state proton transfer.^{129, 137} Study of DHB/valine-proline-leucine (VPL) clusters provided particular insight into the proton transfer event. Although the 3,5 isomer of DHB is 18 kJ/mol more acidic in the gas phase than the 2,5 isomer, it is less able to transfer a proton to VPL in the ionized complex. This is because intermolecular coordination is via the carboxyl group in both cases, which is not the site of the globally most acidic proton. Considering only the carboxyl groups, the 2,5 isomer is indeed more acidic, by 56 kJ/mol. This determines the cluster reactivity since this proton is coordinated to the VPL acceptor. If confirmed by experiment, this would represent an important exception to the general principle that global gas phase thermodynamics can predict MALDI spectra. At the moment it is not clear that such clusters remain in one configuration in the plume, thereby precluding other reaction channels. On the other hand, this result is consistent with the general experience that 3,5 DHB is a much less effective MALDI matrix than the 2,5 isomer.

In spite of the favorable energetics of two-photon complex ionization, it is not believed to be a dominant mechanism in typical practice. This is because the matrix/analyte mole ratio is generally high, 1000 or higher. The bulk of the incoming laser energy is therefore absorbed by the matrix, and matrix-only mechanisms will generate the large majority of ions. Reaction of these primary ions with analyte neutrals dominates over the direct ionization of complexes. Using a modified pooling photoionization model, direct ionization was found to contribute only a few percent to the analyte ion yield, and then only at matrix/analyte >10, and at high fluences.¹⁰²

- Excited state proton transfer (ESPT)

ESPT is an attractive ionization pathway since it can occur in the first electronic excited state, and is therefore a one-photon event with UV excitation. Some molecules undergo a large pK jump upon excitation, of up to 9 units.¹³⁸ Since some MALDI matrices are related to (putative) ESPT molecules like salicylic acid, this has been a recurring

theme.^{3, 139-143, 143, 144} Unfortunately for MALDI, ESPT is highly dependent on an environment which efficiently stabilizes charge separation. Known ESPT systems are often only active in water or amine environments, for example. As noted in the next section, the MALDI plume is not likely to be equally solvating. ESPT molecules have also not generally been very successful in MALDI²⁴ and efforts to find direct indicators of ESPT in matrices like DHB were not successful in either solution or clusters.¹¹⁵ This mechanism therefore appears to be rare, perhaps only active if matrix-analyte complexes are predisposed to proton transfer via strong asymmetric hydrogen bonds and stabilizing neighbor substituents.

- Polar fluid model

In this model^{50, 145} the vaporizing matrix exists for a short time as a dense, polar fluid which behaves like a polar bulk solvent, enabling separation of previously associated ions. For example, a matrix with carboxylic acid groups might liberate protons, which then diffuse in a hydrogen-bonded network to analytes with basic groups. Alternatively, if the analyte itself is acidic or a salt, the fluid could provide an environment suitable for separation of the respective ions.

This picture was originally motivated by the strong qualitative similarity of MALDI spectra regardless of excitation wavelength from the UV to the IR (although the matrix still must have a substantial absorbance). Clearly it would be attractive to have a unified model of UV and IR MALDI, but this similarity need not be a consequence of identical primary ionization mechanisms. As shown above, it is sufficient that secondary reactions are extensive. Then the final ions are simply the most stable, regardless of what the initial primary ions were. Another motivation was occasional observation of analyte ions but no matrix ions in the same spectrum, but this matrix suppression effect has also been shown to be a consequence of secondary reactions.

Although the plume is often a dense fluid for a significant time (at least in the ablation regime, not necessarily in desorption) it is not likely that its properties are sufficiently polar for significant ionization via direct ionic dissociation. Put another way, matrix gas is not sufficiently like water in its solvating abilities. Aromatics with polar substituents tend to have low dielectric constants, around 10 at room temperature (phenol 9.8, methyl salicylate 9.4, acetic acid 6.1).¹⁴⁶ Dielectric constants also drop with temperature, reduction of at least a factor of 2 could be expected at typical plume temperatures. Compare 1-butanol, which has a dielectric constant of 15 at room temperature, but only 7 at 400 C.¹⁴⁶ In such a poorly solvating fluid, autoionization of acidic matrices, or separation of ionic substances will be extremely limited. The energetics of matrix autoionization are addressed below, and the ion yield from such reactions would be too low at MALDI temperatures.¹⁴⁷ Further, the autoionization pK_a of the matrix should determine the ion yield in this model, which must then be the same in IR or UV MALDI for a given matrix. This is not the case, IR yields (ions / neutrals) are about 1000 times lower than in UV.^{145, 148} Such a mechanism would certainly also not be relevant for MALDI with non-polar matrices. Finally, since the plume temperature does not change

dramatically vs. laser fluence,⁵⁶ it is hard to rationalize the high order ionization fluence dependence of MALDI yield in this model.

This is not to say that matrix solvation properties are irrelevant for MALDI. Screening of ions, even with low dielectric constant materials, reduces the range at which Coulomb forces exceed collisional energies, and therefore decreases recombination losses. In this sense the polar fluid picture continues to be a part of modern models such as the MD simulations noted above, but it is not the fundamental basis for ion separation.

- Pneumatic assistance

The pneumatic assistance or expanding bubble model¹⁴⁹⁻¹⁵⁴ may be considered a variant of the cluster model, in that it is based on rapid disintegration of the matrix and associated mechanical separation of preformed ions. The general picture of subsurface nucleation inducing ablation of upper melt layers is also already familiar from the molecular dynamics simulations. It is also similar to the "bubble chamber" model of FAB/SIMS,¹⁵⁵ which apparently traces its ancestry to early ideas of Vestal.¹⁵⁶

In the pneumatic assistance picture, the mechanical force for rapid disintegration is provided by low molecular weight gaseous fragments of matrix, generated by thermal decomposition at typical melt temperatures. This model is therefore not applicable to those matrices which do not efficiently thermally decompose. It could be more widely relevant for IR MALDI, where residual solvent is a ubiquitous source of low molecular weight gas, as well as possibly efficiently absorbing laser energy.¹⁵⁷

Many UV-MALDI matrices are carboxylic acids that thermally decompose, and laser-induced CO₂ emission from matrices in vacuo has been confirmed and measured.¹⁵¹ Rapid gas generation can lead to bubble nucleation and a pressure pulse which causes sample ablation. The bursting of subsurface bubbles creates microdroplets, or clusters and particles in the language of other models.

A quantitative rate equation implementation of the model has been mentioned,^{151, 153, 154} but details have not appeared. The calculated bubble pressure was reported to be 10-100 atm, depending on estimated decomposition rate parameters. This could cause ablation-like cluster ejection at laser fluences which would otherwise induce only smooth desorption. This also leads to a relatively steep dependence of ion yield on fluence, which is a characteristic of MALDI. At fluences which already suffice to ablate matrix without bubbles, decomposition fragments increase the gas pressure by a small factor, around 2, vs. non-decomposing matrices. This is minimal compared to the range of pressures that can be sampled by shortening the laser pulse length, as shown by simulations. Nevertheless, MALDI ion yields are quite similar regardless of pulse length,³²⁻³⁶ so the bubble contribution is apparently not decisive for MALDI, even if it must have some effect for certain matrices.

Secondary Processes

Regardless of whether ions are created free or in clusters or particles, they must become free to be mass-analyzed. Given the large excess of neutral matrix in the (typical) plume, it is therefore nearly always the case that the last intermolecular encounters of an ion are bimolecular collisions with neutral matrix. The possible reactions in these encounters are thus the "bottom line" in defining which ions survive to the detector. This has the fortunate consequence that one generally need not have detailed information concerning reaction cascades in changing particle/cluster and dense plume environments. One example might involve electron transfer:



Others would concern proton transfer (including deprotonated negative ions), or cation transfer. Given approach to local equilibrium under typical conditions, the observed mass spectrum can be predicted from the free energy change of the matrix-analyte and analyte-analyte reactions taking place in the plume, kinetic information is not needed.¹⁵⁸ This useful concept can be tested by inverting the question and verifying that the mass spectrum reflects the reaction thermodynamics according to:

$$\Delta G = -RT \ln(K)$$

Where K is calculated from the relative abundances of ions in the spectrum which are proposed to be involved in charge transfer plume reactions. The reaction free energies are known or can be readily calculated in many cases. Kinsel, et. al have recently performed this test and found excellent agreement for the proton transfer reaction of CHCA matrix to a series of amino acids, as shown in Fig. 6.¹⁵⁹

Fig. 6

Because of near-equilibrium, the observed ion distribution normally remains independent of laser fluence. At low fluence, however, so little material may be released that it expands to the collision-free regime before all reactions approach completion. The mass spectrum is then more reflective of initial primary ions than preferred secondary products. At higher fluence, secondary ions dominate. This fluence-dependent transition has been observed, as seen in Fig. 7 for a simple case.¹⁴⁷ More complex curves are also possible when multiple ion species are involved.¹⁴⁷

Fig. 7

There have been many other, less direct, consequences of the thermodynamic model of the plume which have been successfully tested, but before these are examined it is necessary to consider the types of ions and reactions which should be expected in the plume.

Matrix Ions

Considerable thermodynamic information is now available for several matrices and their various clusters, fragments and ionic forms.^{115, 116, 128-134, 137, 159-167} Experiment

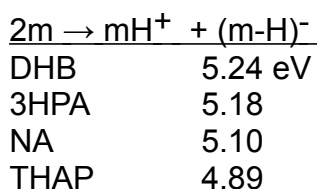
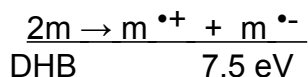
and theory are generally in quite good agreement, and both are represented in Table 1.

Table 1

Matrix ionization potentials were discussed above, and are mostly over 775 kJ/mol. Electron affinities are 100 kJ/mol or less. Neutral matrix proton affinities are 850 to more than 900 kJ/mol ($mH^+ \rightarrow m + H^+$), while the acidities are around 1300 kJ/mol ($m \rightarrow (m-H)^- + H^+$), reflecting the Coulomb contribution. The acidities of the radical cations ($m^{\bullet+} \rightarrow (m-H) + H^+$), are considerably less, about 850 kJ/mol, so electron transfer ionization increases subsequent proton transfer reactivity.

Matrix adducts with alkali cations are often observed. The affinities of neutral matrix for these ions are in the range of 95-105 kJ/mol for K^+ ¹⁶⁸ and 140-170 kJ/mol for Na^+ .^{169, 170}

This information makes it possible to evaluate the autoionization energetics of several matrix ion pairs:



Clearly these are all within the 2-photon range of typical UV lasers. This is not necessarily a photoinduced process, but if autoionization contributes substantially to UV MALDI, it cannot be purely thermal in nature. Otherwise UV and IR MALDI ion yields would be about the same and, as noted above, this is not the case. IR MALDI is about 1000 times less efficient than UV.^{145, 148}

When no analyte is present, a single MALDI event might give rise to strong $m^{\bullet+}$, mH^+ , mNa^+ , $m^{\bullet-}$, and $(m-H)^-$ signals. In addition various thermal or non-thermal decay products of the matrix might be formed, such as $m-H_2O$, or $m-CO_2$. Further, depending on the matrix, rather surprising species are sometimes found, such as $(m-nH)^+$, or $(m+2H)^+$. These are seldom dominant, but clearly present. In addition, rather unusual species have been identified in the plume, such as H atoms,¹⁷¹ which make the existence of radicals like $(m-H)^{\bullet}$ likely, although these and similar species can also be generated by dissociative electron capture.^{100, 172} Some of these reactions may be highly analogous to those proposed for SIMS.^{173, 174}

In the dense plume, the various ion types, which seem at first glance to be independent classes, must interconvert if local equilibrium is to be achieved. It has been shown for DHB that interconversion of m^+ , mH^+ and mNa^+ is thermally possible under typical plume conditions.^{130, 158} These reactions are mediated by neutral matrix. Although the protonated matrix is the most stable in this case, the energy needed to reach the other ion types may be as low as 30 kJ/mol, well within kT in the plume. This would explain why all may be observed in the mass spectrum at the same time. A similar situation apparently holds for many other matrices, as will be shown from the matrix suppression effect.

Matrix-Analyte, Analyte-Analyte Reactions and Suppression Effects

Matrix Suppression Effect

One of the more dramatic MALDI phenomena, and one which clearly points to extensive matrix-analyte reactions is the matrix suppression effect (MSE). It was sporadically noted,^{95, 175, 176} but the full implications were not realized until it was placed in the context of the two step picture and interpreted as a consequence of secondary reactions.^{177, 178}

As the name implies, matrix ions can be completely suppressed by analytes at appropriate concentration ratios, as shown in Fig. 8. It is a rather general phenomenon,¹⁷⁹ and suppression includes all matrix ions, not only protonated or cationized matrix or radical cations. This observation shows the connection to secondary reactions. If, for example a strongly basic analyte depletes protonated primary matrix ions, depletion of other matrix ions must occur via interconversion, as noted above.

Fig. 8

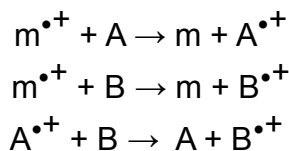
Note that the preformed/cluster model cannot explain the MSE, even though it includes secondary reactions in clusters. In that picture preformed matrix ions can donate their charge to analytes in the same cluster, if any are available, and the reaction is favorable.³⁰ However, attaining MSE would then require that there are *never* more charges than analyte molecules in *any* randomly formed cluster- a statistical impossibility, especially since the analyte is known to be unevenly distributed on a macroscopic scale in many MALDI samples.¹⁸⁰⁻¹⁸³ In the gas, mobility is much higher than in clusters, so mixing is comparatively good, and minor sample inhomogeneities less relevant. Combining this mixing with the interconversion reactions above, a straightforward explanation emerges for the MSE.

If the analyte reacts efficiently with matrix ions of one polarity, it is unlikely (but not impossible) that reaction in the opposite polarity will also be favorable. As a result MSE typically appears only in one polarity. The polarity of MSE is usually easily predicted. Basic analytes strongly deplete protonated matrix, for example, so suppression occurs in positive mode, but all predictions must use gas-phase properties, not solution phase. For full suppression, it is necessary that sufficient analyte be present to react with all primary matrix ions. The MSE is therefore concentration dependent, as well as dependent on the laser fluence (concentration of primary ions). Further characteristics of

the MSE will be discussed below in connection with detailed models.

Analyte Suppression Effect

Secondary reactions modify not only the matrix signal in the presence of one analyte, but can also strongly affect the relative intensities of multiple analytes. Consider the case where analytes A and B are present. They can undergo reaction with matrix ions, and with each other:



There are then two pathways for analyte-analyte suppression: First, if B reacts more efficiently with $m^{\bullet+}$ than A, then $A^{\bullet+}$ will appear less strongly than it would in the absence of B. Second, charge transfer reactions may take place directly between analytes. Note that ASE implies sufficient analyte to deplete matrix (otherwise both of the top reactions can occur), so ASE is accompanied by MSE. An example of both effects is shown in Fig. 9.

Fig. 9

Once again, the ion types are unimportant if matrix interconversion reactions are facile, so it is possible to observe suppression of one type of analyte ion by another. ¹⁵⁸

The ASE is merely the most extreme example of a general problem in MALDI, that of varying sensitivity factors for analytes depending on the nature of the mixture under study. The secondary ionization model shows us what parameters are important in understanding and controlling these effects: the reaction exothermicities (and possibly kinetics) of the various charge transfer reactions, and the relative concentrations of the reactants. These will be quantitatively revisited below, but first it is necessary to expand on matrix-analyte reactions.

Proton Transfer

One of the most important applications of MALDI is to protein and peptide analysis, these are typically observed as protonated molecules. Gas-phase proton affinities for amino acids range from 885 kJ/mol for glycine to 1025 kJ/mol for arginine.¹⁸⁴ As seen from Table 1, proton transfer from typical matrices to glycine will be weakly exothermic to endothermic, while arginine can easily abstract a proton from all. This reflects the common experience that peptides containing more basic residues are preferentially observed in MALDI (even if basicity is not the sole factor).¹⁸⁵⁻¹⁸⁹ In addition multiple coordination of attached protons increases the total affinity.^{184, 190-192} In contrast, oligonucleotides are weakly basic and measured much more readily in negative polarity as deprotonated molecules.¹⁹³ In this case it is the comparatively high proton affinity of deprotonated matrix anions which gives high analyte anion yield.

Cationization

Proton transfer reactions of analytes with matrix are often the most exoergic available, and determine the ions observed. This is not always the case, and there are major analyte classes, most notably synthetic polymers, which are often better analyzed as other adducts, typically with alkali (e.g. Na^+ , K^+) or transition metal (e.g. Cu^+ , Ag^+) cations. Since these substances may have no polar groups, it is not surprising that proton affinities or acidities can be lower than those of most matrices. At the same time, there may be good affinity for some cations, transition metal ions may make relatively strong d- π complexes with aromatic side chains, for example.¹⁹⁴

Sodium affinities of common matrices are in the range of 140-170 kJ/mol, while for most amino acids they are above 150 kJ/mol (for dipeptides >160).¹⁹⁵⁻¹⁹⁷ Affinities of both nucleobases and carbohydrates lie higher, 164-190 and >160 kJ/mol, respectively.¹⁹⁵ From this we can conclude that analyte- Na^+ complex formation may or may not be competitive with the corresponding matrix reaction. Or to put it another way, one should choose a matrix with a low cation affinity to significantly enhance analyte cationization. Dithranol (1,8 dihydroxyanthrone), for example, has become favored for polymer analysis, and has been found to have a cation affinity below that of sinapinic acid, DHB and THAP. Other matrices also show trends in cationization, suppression and other behaviors which are consistent with the thermodynamics of cation transfer.^{25, 198}

Since cationization obviously requires presence of the corresponding cations in the sample, the question of preformed ions is more acute than with de/protonation, which can occur without additives. Several studies support a predominantly gas-phase process,^{94, 96, 199-201} but this remains a difficult topic to investigate in a decisive manner.²⁰² The MALDI efficiency of finely ground (but not cocrystallized) matrix and analyte^{203, 204} may also point to plume cationization. To whatever extent preformed ions exist, their stability in the plume, and hence appearance in the mass spectrum, remains determined by reactivity in collisions with matrix, so the spectrum should remain predictable using gas-phase thermodynamics.

Adding an appropriate salt to MALDI samples can increase analyte adduct signal substantially, if these cations are not naturally present (commercial matrix is often significantly contaminated with salts²⁰⁵). Adding excess of one cation can also simplify the spectrum by ensuring dominant ionization with the desired cation, if several are naturally present.

Too much salt can lead to signal loss, often due to crystallization effects that vary with preparation method,^{205, 206} or due to dilution of matrix. Ideally then, the optimum amount of salt would be stoichiometrically equivalent to the amount of analyte. Unfortunately, competition of matrix and analyte for cations can necessitate above-stoichiometric salt quantities for strongest analyte signal, especially when deprotonated matrix is expected for many matrices via the photochemical mechanism. Since $(\text{m-H})^-$ will have a higher cation affinity than all neutral molecules, it efficiently reduces the amount of cation available for analytes.²⁰⁷ Neutral matrix is also a competitor, as can

be directly verified by observation of matrix adducts in the spectrum.²⁰⁵

Electron Transfer

The third main type of ion observed in MALDI after de/protonated or cationized species is the radical cation or anion.²⁰⁸⁻²¹³ While matrix radical ions are not uncommon, analyte radicals are unusually only observed for low polarity molecules with few or no functional groups.

Electron transfer (ET) from neutral analytes to matrix ions is the secondary step leading to radical analyte cations.^{209, 210} The difference in ionization potentials (IPs) of matrix and analyte or between analytes is the relevant thermodynamic parameter explaining the features of the mass spectra.²¹⁰ An analogous picture has been demonstrated for generation of radical anions of fullerene derivatives in LDI and MALDI.^{211, 214} The corresponding quantity in negative polarity is the difference in electron affinities. It was also shown that the matrix-analyte ET exoergicity is strongly correlated with fragmentation of fluorofullerenes.²¹¹

As seen in Fig. 9, ET reactions lead to the same kind of suppression phenomena (MSE and ASE) due to secondary reactions as are known from protonation and cationization. The only unusual aspect found so far is that ET reactions between partners with very different ionization potentials (difference > 1.5 eV) appear to become rather slow, to the point that the reaction is incomplete on the MALDI time scale.¹¹⁶ This raises the question of a kinetic effect similar to Marcus inversion,²¹⁵ but many questions remain regarding gas-phase electron transfer reactions, especially regarding encounter complex formation. Matrix choice becomes more difficult in this situation, since it must have a higher IP than all analytes, but not more than about 1.5 eV above the lowest IP analyte.

One kind of ET that is frequent in MALDI concerns multivalent cations. Salts of Ca^{2+} , Cu^{2+} or similar cationizing agent can be added to the sample, but only singly charged adducts are observed. The metal ions are reduced to +1,^{85, 97, 216-218} or H^+ is ejected from the complex.^{219, 220} This can be understood from the electrostatic energy of multiple charges on a single molecule in the gas phase. This is highest when the charge is concentrated on the cation itself. The first IP of Cu ($\text{Cu} \rightarrow \text{Cu}^+$) is 7.7 eV while the second ($\text{Cu}^+ \rightarrow \text{Cu}^{2+}$) is 20.3 eV.²²¹ Reaction with neutral matrix (IP about 8 eV) can reduce the metal to the +1 state, but not neutralize it. In the other route, H^+ ejection, the excess charge is exported in a different way, but the net effect is to transfer an electron to the M^{2+} site, again reducing it to +1. The approximately 10 eV decrease in electrostatic energy is far more than enough to compensate for the loss of a R-H covalent bond.

Multiply Charged Analytes

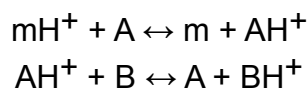
Similar to the reduction of multivalent cations, the prevalence of multiply charged ions of all types should be predictable from their stability with respect to plume reactions. The higher the charge state, the more difficult it is to create because of internal electrostatic

energy. This is reflected in the basicities of biomolecules, which drop steadily and steeply as a function of increasing prior protonation.²²² The internal repulsion energy of a multiply charged ion is decreased if the charges can be widely separated, so the MALDI tendency to generate +2 or higher charge states increases with molecular size.

For multiply protonated analytes, the available data is consistent with limitation of charge state via exothermic H⁺ abstraction by matrix.^{158, 191, 223, 224} The lower limit for dual protonation of peptides has been estimated to require a separation of >0.9 nm between protonation sites,¹⁵⁸ similar to that of gramicidin S.²²⁵ Multiple charging may also be kinetically limited even if thermodynamically favorable,¹⁰⁸ as noted above in the discussion of the cluster model.

The Quantitative 2-Step Model Including Analyte

There is currently only one comprehensive MALDI model capable of quantitative predictions of matrix and analyte ion yields, and which includes experimentally relevant factors such as laser characteristics, matrix/analyte ratio, and physical and chemical properties of matrix and analyte.²²⁶ This model builds on the matrix-only pooling model noted above,⁶⁰ and therefore assumes that primary ions are derived only from matrix. Analyte signal is solely a consequence of secondary reactions:



The rates were taken to have Arrhenius form, and the activation energies were derived from non-linear free energy relationships developed for proton transfer reactions.^{227, 228} This is the only aspect of the model which specifies the ion type, otherwise it is general. The activation energy is highest at low reaction free energy, dropping to near zero for large exoergicity, above 60-90 kJ/mol. The Arrhenius prefactor is the hard-sphere collision rate, which introduces an analyte molecular weight dependence into the secondary rates via the molecular radius, which was obtained from ion mobility studies.

A positive feature of this model is that it has no adjustable parameters. The properties of matrix, analytes and laser fully define the result. The necessary matrix parameters are well-determined quantities such as proton affinities, making the secondary aspect of the model applicable to many matrices, not only DHB. A number of experimental phenomena are well reproduced as is briefly summarized next.

The matrix suppression effect is well reproduced, as shown in Fig. 7 & 8, as a function of matrix/analyte ratio, reaction exoergicity, and laser fluence.¹⁷⁷ The MSE also occurs at a lower concentration for high molecular weight analytes,¹⁷⁸ because bigger molecules have a higher probability of collision with primary matrix ions.

The analyte suppression effect is also correctly predicted as a function of secondary reaction exothermicities. The dependence of relative analyte signals on matrix/analyte

ratio compares well with experimental examples.¹⁵⁸ Analyte intensity ratios can be brought closer to the concentration ratios in the sample by generating more primary ions at higher fluence, but this does not reach the correct values at any fluence.¹¹⁶ Because of the size-dependent collision probabilities, analytes of similar reactivity but different molecular weight may exhibit different intensities, as has recently been shown experimentally.¹⁸⁹

Since both the MSE and ASE are dependent on secondary reaction free energies, highly exothermic reactions like proton transfer more readily induce suppression (it appears at lower analyte concentration) than do less energetic reactions like cation transfer.

There is a 2-pulse time delay effect for analytes as well as matrix, but a delayed maximum was not found for analytes.²²⁹ The model gives quantitative agreement with the data.²²⁶

Some practical implications of the model involving the choices available in a MALDI experiment are implied in these results, but worth describing explicitly. Most importantly, the response factor for each analyte depends significantly on the other analytes, and the suppression can be predicted by the thermodynamics of the corresponding secondary reactions. Responses also depend on analyte/analyte concentration ratios and the ratio of total analyte to matrix. Generally, dilution with matrix leads to a better relative intensities, at a cost in overall sensitivity. The response factor for any analyte will be higher, more stable and more reproducible if it is the one which has the most favorable secondary reaction thermodynamics.

Increasing the quantity of primary matrix ions by increasing the laser intensity reduces selective suppression effects, giving more accurate intensity ratios. This is an advantage for atmospheric pressure MALDI over vacuum MALDI-ToF, where mass resolution suffers from an extremely dense plume at high fluences.

Favorable plume reactions (producing strong analyte signals) depend on matrix choice. There is now enough thermodynamic information available on matrices that it should seldom be necessary to try them at random, if analyte properties are known or can be estimated. Similarly, cationization can also be strategically planned, based on knowledge of the analyte and which cations might better bind to it compared to the chosen matrix.

Surface Effects

While the main thrust of MALDI mechanistic investigation has been directed toward bulk samples, the sample support can affect the experimental outcome if the sample is thin enough. Because this can involve the matrix itself, this relatively new research topic is briefly mentioned here. Note that this does not include particle substrate or nanostructured surface methods, since the substrate dependence in those cases may be more due to thermal effects, not ionization behavior involving matrix.

The penetration depth of typical lasers in UV matrices is no more than a few 100 nm,⁵⁹ so this is the upper sample thickness limit for direct laser effects involving the substrate.

Sample morphology is known to affect MALDI response,^{183, 230-232} possibly by modifying desorption/ablation behavior, so surface-induced modification of matrix crystal habit may be a complicating factor. However, this does not seem to be an issue for comparison of metal substrates.²³³

Free electrons are central to the lucky survivor model. Recently it has also been reported that electrons from the metal under thin samples reduce positive ion yield.²³⁴ Yield was also reported to be better from a gold substrate vs. stainless steel, due to differences in the photoelectron energy and capture cross section.²³⁵ From measured matrix capture cross sections,¹⁷² the mean free path of low energy electrons, around 1 eV, is on the order of 10-50 nm. For this type of substrate effect "thin" must therefore refer to layers of less than about 100 nm. The samples in these studies were made by the dried drop method, however, and so did not have a uniform thickness. They were characterized as "thin" if a closed surface of matrix crystals was not formed. The areas between the macroscopic crystals was taken to be covered in a very thin matrix layer.

Matrix on the surface is proposed to dramatically lower the work function of the metal so that 1-photon photoemission becomes possible.²³⁵ The required decrease is as much as 2 eV versus the bare, clean metal. Such reductions have not been previously reported in well controlled experiments.²³⁶ Reductions of less than 1 eV are much more typical, especially if the metal was not extensively cleaned in ultra high vacuum beforehand.²³⁷ Electron yield measurements²³⁵ were interpreted as supporting 1-photon emission,²³⁸ but were later shown to be better reproduced by a model which includes pooling and sequential two-photon ionization. 102, 235, 239

Compared to dried drops, good control of sample thickness is provided by electrospray deposition. Recent MALDI/ToF imaging studies of electrosprayed DHB spots down to a few 100 nm thickness have shown dramatic enhancements (not reductions) of matrix and analyte signals for the last layers near a stainless steel substrate surface.^{233, 239} Drilling experiments and varying the laser power to achieve partial or total ablation corroborated increased ionization efficiency for the last layers near the steel. The images showed that the enhancement was greatest in the thinnest parts of the samples. Example images are shown in Fig. 10.

Fig 10 sprayed spots

A gold substrate gave a much smaller enhancement, which is consistent with a two-photon ionization model based on interaction of matrix orbitals with the conduction band of the metal. The ion yield vs. laser fluence was quantitatively shown to predict the yield of thick vs. thin samples.²³³ Consistent results were obtained over many samples and over many points on each sample.

The apparent conflict between reports of enhancement vs. suppression of MALDI signal from thin samples on metals may be partly associated with instrumental methods. The experiments showing suppression were mostly (but not entirely) performed with an in-

magnet FT-ICR source. Those showing enhancement were all performed in ToF instruments. In the magnet, charged species are confined to the same magnetic field lines, which increases the probability of recombination compared to the ToF, where ions are rapidly separated by polarity.

It is not necessary for the metal-matrix interface to be at the bottom of the sample. A thin metal layer can be sputter-coated on the top of a normal MALDI sample as well.²⁴⁰ Much of the benefit of a toplayer is no doubt associated with reduced surface charging of insulating samples, but probably not all. The layer needs to be very thin, so that laser light reaches the underlying matrix. Nominal thickness are usually a few nm, but the metal may form islands which aid desorption.²⁴¹ Gold is easy to sputter, and moderate enhancement effects similar to a gold underlayer were observed.²³³

Summary and Outlook

The two step framework for UV-MALDI ionization, especially the concept of extensive secondary reactions in the dense plume, is gaining acceptance. The primary ionization step remains somewhat controversial, but the range of opinion is less wide than just a few years ago. There are now two main viewpoints: one advocating preformed ions in clusters and one advocating (pooling-mediated) photoionization of matrix. The pooling/photoionization picture has been coupled with a model for the plume expansion, leading to quantitative predictions for many observables. While only the matrix 2,5 DHB is currently modeled in detail, other matrices behave similarly in many respects, suggesting that the basic concepts could be more general.

Understanding of the secondary reactions in MALDI has developed considerably in recent years. The recognition that local equilibrium often is approached in the plume has made it increasingly important to measure gas-phase thermodynamic properties of matrices and analytes, since these have a major, even definitive, impact on the final spectrum. Secondary reactions, which are dominated by the matrix as the most common collision partner, also lead to a certain commonality of MALDI behavior for all ion types.

Mechanistic theory and models are helping to better understand those factors influencing relative and absolute analyte signal intensities, and where the limits of MALDI may lie. For example it cannot be expected that uniform response for all peptides in a protein digest will be achieved using a typical MALDI preparation. On the other hand, quantitation appears to be fundamentally and generally possible, but subject to significant potential complications depending on the range of substances present, both in concentration and type.

Seen as a kind of chemical ionization process, MALDI applications can usually be addressed by asking what are the gas-phase thermodynamics of the possible reactions in the plume, and how much of the reactants are available. Better analytical results will be obtained by making experimental choices that favor formation of the desired analyte ions over other potential competitors.

That practically applicable frameworks for planning and interpreting UV-MALDI experiments exist is a step forward. This is not, however, to imply that MALDI

mechanisms are fully known. There are numerous indications that many unusual species and processes are involved, so the current picture of plume reactions may be too simple. For example, unexpected or unexplained ions are often found in MALDI spectra, but fortunately these are not typically dominant. There are also undoubtedly interesting neutrals involved, they are simply silent in the mass spectrum. Only relatively few matrix molecules have been extensively characterized, none as fully as could be desired, and it is still not clear why one matrix is good and another not. Only 2,5-DHB is known sufficiently to be used in quantitative models of primary ionization, although the secondary reactivities and thermodynamic properties of several others are well studied. Strongly oriented matrix-analyte complexes may significantly modify or limit the available ionization reaction channels. The chemical physics of the coupled phase change, primary ionization and subsequent expanding, reacting, hot material are still under active investigation. The ternary systems used in polymer analysis (matrix, polydisperse analyte and cationizing reagent) are also a continuing challenge.

In short, understanding of UV-MALDI ionization has advanced past an empirical, descriptive phase, and can aid in practical applications, but there is still much to be learned about this complex and multifaceted method.

Acknowledgments

The author thanks A. Hotelling for careful reading of the manuscript and insightful suggestions.

Literature Cited

1. M. Yamashita, J. B. Fenn, *J. Phys. Chem.* **88**, 4671 (1984).
2. M. Karas, D. Bachmann, F. Hillenkamp, *Anal. Chem.* **57**, 2935 (1985).
3. M. Karas, D. Bachmann, U. Bahr, F. Hillenkamp, *Int. J. Mass Spectrom. Ion Proc.* **78**, 53 (1987).
4. M. Karas, F. Hillenkamp, *Anal. Chem.* **60**, 2299 (1988).
5. R. B. Cole, *J. Mass Spectrom.* **35**, 763 (2000).
6. P. Kebarle, *J. Mass Spectrom.* **35**, 804 (2000).
7. J. Sunner, I. B. Beech, K. Hiraoka, *J. Am. Soc. Mass Spectrom.* **17**, 151 (2006).
8. M. C. Fitzgerald, G. R. Parr, L. M. Smith, *Anal. Chem.* **65**, 3204 (1993).
9. K. J. Wu, A. Steding, C. H. Becker, *Rapid Commun. Mass Spectrom.* **7**, 142 (1993).
10. R. C. Beavis, B. T. Chait, *Rapid Commun. Mass Spectrom.* **3**, 233 (1989).
11. P. Juhasz, C. E. Costello, K. Biemann, *J. Am. Soc. Mass Spectrom.* **4**, 399 (1993).
12. U. Pieleles, W. Zürcher, M. Schär, H. Moser, *Nucl. Acid Res.* **21**, 3191 (1993).
13. K. Strupat, M. Karas, F. Hillenkamp, *Int. J. Mass Spectrom. Ion Proc.* **111**, 89 (1991).
14. R. C. Beavis, T. Chaudary, B. T. Chait, *Org. Mass Spectrom.* **27**, 156 (1992).
15. D. W. Armstrong, L.-K. Zhang, L. He, M. L. Gross, *Anal. Chem.* **73**, 3679 (2001).
16. M. Zabet-Moghaddam, E. Heinzle, A. Tholey, *Rapid Commun. Mass Spectrom.* **18**, 141 (2004).
17. K. Tanaka, H. Waki, Y. Ido, S. Akita, Y. Yoshida, T. Yoshida, *Rapid Commun. Mass Spectrom.* **2**, 151 (1988).
18. J. Wei, J. M. Burlak, G. Siuzdak, *Nature* **399**, 243 (1999).
19. G. E.P., J. V. Apon, G. Luo, A. Saghatellan, R. H. Daniels, V. Sahl, R. Dubrow, B. F. Cravatt, A. Vertes, G. Siuzdak, *Anal. Chem.* **77**, 1641 (2005).
20. R. Zenobi, R. Knochenmuss, *Mass Spectrom. Rev.* **17**, 337 (1998).
21. F. Hillenkamp, *Springer Series in Chemical Physics vol. 25*, 190 (1983).
22. F. Hillenkamp, M. Karas, R. C. Beavis, B. T. Chait, *Anal. Chem.* **63**, 1193A (1991).
23. M. Karas, U. Bahr, U. Giessmann, *Mass Spectrom. Rev.* **10**, 335 (1991).
24. H. Ehring, M. Karas, F. Hillenkamp, *Org. Mass Spectrom.* **27**, 427 (1992).
25. P.-C. Liao, J. Allison, *J. Mass Spectrom.* **30**, 408 (1995).
26. M. Karas, U. Bahr, J.-R. Stahl-Zeng, **Large Ions: Their Vaporization, Detection and Structural Analysis**, 27 (1996).
27. R. G. Cooks, K. L. Busch, *Int. J. Mass Spectrom. Ion Phys.* **53**, 111 (1983).
28. L. V. Zhigilei, E. Leveugle, B. J. Garrison, Y. G. Yingling, M. I. Zeifman, *Chem. Rev.* **103**, 321 (2003).
29. K. Dreisewerd, *Chem. Rev.* **103**, 395 (2003).
30. M. Karas, R. Krüger, *Chem. Rev.* **103**, 427 (2003).
31. R. Knochenmuss, R. Zenobi, *Chem. Rev.* **103**, 441 (2003).
32. P. Demirev, A. Westman, C. T. Reimann, P. Håkansson, D. Barofsky, B. U. R. Sundqvist, Y. D. Cheng, W. Seibt, K. Siegbahn, *Rapid Commun. Mass Spectrom.* **6**, 187 (1992).
33. K. Dreisewerd, M. Schürenberg, M. Karas, F. Hillenkamp, *Int. J. Mass Spectrom. Ion Proc.* **154**, 171 (1996).
34. M. R. Chevrier, R. J. Cotter, *Rapid Commun. Mass Spectrom.* **5**, 611 (1991).

35. M. R. Papantonakis, J. Kim, W. P. Hess, R. F. Haglund, *J. Mass Spectrom.* **37**, 639 (2002).
36. A. Meffert, J. Grotemeyer, *Int. J. Mass Spectrom.* **210/211**, 521 (2001).
37. C. Zechmann, T. Muskat, J. Grotemeyer, *Eur. J. Mass Spectrom.* **8**, 287 (2002).
38. H.-C. Lüdemann, R. W. Redmond, F. Hillenkamp, *Rapid Comm. Mass Spectrom.* **16**, 1287 (2002).
39. P. Setz, R. Knochenmuss, *J. Phys. Chem. A* **109**, 4030 (2005).
40. L. V. Zhigilei, P. B. S. Kodali, B. J. Garrison, *J. Phys. Chem. B* **101**, 2028 (1997).
41. L. V. Zhigilei, P. B. S. Kodali, B. J. Garrison, *J. Phys. Chem. B* **102**, 2845 (1998).
42. L. V. Zhigilei, B. J. Garrison, *J. Appl. Phys.* **88**, 1 (2000).
43. L. V. Zhigilei, *Appl. Phys. A* **76**, 339 (2003).
44. S. Kristyan, A. Bencsura, A. Vertes, *Theor. Chem. Acc.* **107**, 319 (2002).
45. A. A. Poretzky, D. B. Geohegan, *Chem. Phys. Lett.* **286**, 425 (1997).
46. M. Handschuh, S. Nettesheim, R. Zenobi, *Appl. Surf. Sci.* **137**, 125 (1998).
47. S. N. Jackson, S. Mishra, K. K. Murray, *J. Phys. Chem. B* **107**, 13106 (2003).
48. S. Alves, M. Kalberer, R. Zenobi, *Rapid Comm. Mass Spectrom.* **17**, 2034 (2003).
49. E. Stevenson, K. Breuker, R. Zenobi, *J. Mass Spectrom.* **35**, 1035 (2000).
50. X. Chen, J. A. Carroll, R. C. Beavis, *J. Am. Soc. Mass Spectrom.* **9**, 885 (1998).
51. M. Schuerenberg, K. Dreisewerd, S. Kamanabrou, F. Hillenkamp, *Int. J. Mass Spectrom.* **172**, 89 (1998).
52. W. E. Wallace, M. A. Arnould, R. Knochenmuss, *Int. J. Mass Spectrom.* **242**, 13 (2005).
53. D. M. Price, S. Bashir, P. R. Derrick, *Thermochim. Acta* **327**, 167 (1999).
54. C. D. Mowry, M. V. Johnston, *J. Phys. Chem.* **98**, 1904 (1994).
55. K. Dreisewerd, M. Schürenberg, M. Karas, F. Hillenkamp, *Int. J. Mass Spectrom. Ion Proc.* **141**, 127 (1995).
56. G. Luo, I. Marginean, A. Vertes, *Anal. Chem.* **74**, 6185 (2002).
57. V. Gabelica, Schulz, E, M. Karas, *J. Mass Spectrom.* **39**, 579 (2004).
58. A. Koubenakis, V. Frankevich, J. Zhang, R. Zenobi, *J. Phys. Chem. A* **108**, 2405 (2004).
59. R. Knochenmuss, L. V. Zhigilei, *J. Phys. Chem. B* **109**, 22947 (2005).
60. R. Knochenmuss, *J. Mass Spectrom.* **37**, 867 (2002).
61. R. C. Beavis, B. T. Chait, *Chem. Phys. Lett.* **181**, 479 (1991).
62. D. R. Miller, **Atomic and Molecular Beam Methods** **1**, 14 (1988).
63. A. Vertes, L. Balazs, R. Gijbels, *Rapid Commun. Mass Spectrom.* **4**, 263 (1990).
64. A. Vertes, G. Irinyi, R. Gijbels, *Anal. Chem.* **65**, 2389 (1993).
65. A. Bencsura, A. Vertes, *Chem. Phys. Lett.* **247**, 142 (1995).
66. A. Bencsura, V. Navale, M. Sadeghi, A. Vertes, *Rapid Commun. Mass Spectrom.* **11**, 679 (1997).
67. I. Fournier, C. Marinach, J.-C. Tabet, G. Bolbach, *J. Am. Soc. Mass Spectrom.* **14**, 893 (2003).
68. I. Fournier, J.-C. Tabet, G. Bolbach, *Int. J. Mass Spectrom.* **219**, 515 (2002).
69. M. Sadeghi, X. Wu, A. Vertes, *J. Phys. Chem. B* **105**, 2578 (2001).
70. E. Leveugle, D. S. Ivanov, L. V. Zhigilei, *Appl. Phys. A* **79**, 1643 (2004).
71. Y. G. Yingling, L. V. Zhigilei, B. J. Garrison, *J. Photochem. Photobiol. A* **145**, 173 (2001).
72. L. V. Zhigilei, Y. G. Yingling, T. E. Itina, T. A. Schoolcraft, B. J. Garrison, *Int. J. Mass Spectrom.* **226**, 85 (2003).

73. Y. G. Yingling, B. J. Garrison, *J. Phys. Chem. B* **108**, 1815 (2004).
74. C. Jouvet, C. Lardeux-Dedonder, M. Richard-Viard, D. Solgadi, A. Tramer, *J. Phys. Chem.* **94**, 5041 (1990).
75. T. Huth-Fehre, C. H. Becker, *Rapid Commun. Mass Spectrom.* **5**, 378 (1991).
76. Y. Pan, R. J. Cotter, *Org. Mass Spectrom.* **27**, 3 (1992).
77. B. Spengler, V. Bökelmann, *Nucl. Instr. Meth. Phys. Res. B* **82**, 379 (1993).
78. P. Juhasz, M. L. Vestal, S. A. Martin, *J. Am. Soc. Mass Spectrom.* **8**, 209 (1997).
79. M. Glückmann, M. Karas, *47th ASMS Conference on Mass Spectrometry and Allied Topics* 2232 (1999).
80. M. Glückmann, M. Karas, *J. Mass Spectrom.* **34**, 467 (1999).
81. J. Zhou, W. Ens, K. G. Standing, A. Verentchikov, *Rapid Commun. Mass Spectrom.* **6**, 671 (1992).
82. M. Karas, M. Glückmann, J. Schäfer, *J. Mass Spectrom.* **35**, 1 (2000).
83. R. Krüger, A. Pfenninger, I. Fournier, M. Glückmann, M. Karas, *Anal. Chem.* **73**, (2001).
84. P.-C. Liao, J. Allison, *J. Mass Spectrom.* **30**, 511 (1995).
85. E. Lehmann, R. Knochenmuss, R. Zenobi, *Rapid Commun. Mass Spectrom.* **11**, 1483 (1997).
86. J. Claereboudt, M. Claeys, H. Geise, R. Gijbels, A. Vertes, *J. Am. Soc. Mass Spectrom.* **4**, 798 (1993).
87. I. G. Gut, W. A. Jeffery, D. J. C. Pappin, S. Beck, *Rapid Commun. Mass Spectrom.* **11**, 43 (1997).
88. T. J. P. Naven, D. J. Harvey, *Rapid Commun. Mass Spectrom.* **10**, 829 (1996).
89. B. Spengler, F. Lützenkirchen, S. Metzger, P. Chaurand, R. Kaufmann, W. Jeffery, M. Bartlett-Jones, D. J. C. Pappin, *Int. J. Mass Spectrom. Ion Proc.* **169/170**, 127 (1997).
90. J. M. Asara, J. Allison, *Anal. Chem.* **71**, 2866 (1999).
91. J. R. Strahler, Y. Smelyanskiy, G. Lavine, J. Allison, *Int. J. Mass Spectrom. Ion Proc.* **169/170**, 111 (1997).
92. K. Berlin, I. G. Gut, *Rapid Commun. Mass Spectrom.* **13**, 1739 (1999).
93. F. L. Brancia, S. G. Oliver, S. J. Gaskell, *Rapid Commun. Mass Spectrom.* **14**, 2070 (2000).
94. A.-M. Hoberg, D. M. Haddleton, P. M. Derrick, *Eur. Mass Spectrom.* **3**, 471 (1997).
95. V. Bökelmann, B. Spengler, R. Kaufmann, *Eur. Mass Spectrom.* **1**, 81 (1995).
96. P. C. Burgers, J. K. Terlouw, *Rapid Commun. Mass Spectrom.* **12**, 801 (1998).
97. M. J. Deery, J. K., C. B. Jasieczek, D. M. Haddleton, A. T. Jackson, H. T. Yates, J. H. Scrivens, *Rapid Commun. Mass Spectrom.* **11**, 57 (1997).
98. H. Ehring, C. Costa, P. A. Demirev, B. U. R. Sundqvist, *Rapid Commun. Mass Spectrom.* **10**, 821 (1996).
99. M. Haisa, S. Kashino, S.-I. Hanada, K. Tanaka, S. Okazaki, M. Shibagaki, *Acta Cryst.* **B38**, 1480 (1982).
100. S. A. Pshenichnyuk, N. L. Asfandiarov, V. S. Fal'ko, V. G. Lukin, *Int. J. Mass Spectrom.* **227**, 281 (2003).
101. S. A. Pshenichnyuk, N. L. Asfandiarov, V. S. Fal'ko, V. G. Lukin, *Int. J. Mass Spectrom.* **227**, 259 (2003).
102. R. Knochenmuss, *Anal. Chem.* **76**, 3179 (2004).
103. G. R. Kinsel, R. D. Edmondson, D. H. Russell, *J. Mass Spectrom.* **32**, 714 (1997).
104. G. R. Kinsel, M. E. Gimon-Kinsel, K. J. Gillig, D. H. Russell, *J. Mass Spectrom.*

34, 684 (1999).

105. A. N. Krutchinsky, B. T. Chait, *J. Am. Soc. Mass Spectrom.* **13**, 129 (2002).
106. I. Fournier, A. Brunot, J.-C. Tabet, G. Bolbach, *Int. J. Mass Spectrom.* **213**, 203 (2002).
107. I. Fournier, A. Brunot, J.-C. Tabet, G. Bolbach, *J. Mass Spectrom.* **40**, 50 (2005).
108. S. Alves, I. Fournier, C. Afonso, F. Wind, J.-C. Tabet, *Eur. J. Mass Spectrom.* **submitted**, (2006).
109. S. Mukamel, D. Abramavicius, *Chem. Rev.* **104**, 2073 (2004).
110. Dexter; D. L.; Knox; R. S. *Excitons*; John Wiley & Sons: New York, 1965;
111. Birks; J. B. *Photophysics of Aromatic Compounds*; Wiley Interscience: London, 1970;
112. Birks; J. B. *Organic Molecular Photophysics*; Wiley: New York, 1973;
113. H. Ehring, B. U. R. Sundqvist, *J. Mass Spectrom.* **30**, 1303 (1995).
114. H. Ehring, B. U. R. Sundqvist, *Appl. Surf. Sci.* **96-8**, 577 (1996).
115. V. Karbach, R. Knochenmuss, *Rapid Commun. Mass Spectrom.* **12**, 968 (1998).
116. A. J. Hoteling, W. F. Nichols, D. J. Giesen, J. R. Lenhard, R. Knochenmuss, *Eur. J. Mass Spectrom.* **submitted**, (2006).
117. R. Knochenmuss, A. Vertes, *J. Phys. Chem. B* **104**, 5406 (2000).
118. C. Mowry, M. Johnston, *Rapid Comm. Mass Spectrom.* **7**, 569 (1993).
119. A. P. Quist, T. Huth-Fehre, B. U. R. Sunqvist, *Rapid Commun. Mass Spectrom.* **8**, 149 (1994).
120. W. Ens, Y. Mao, F. Mayer, K. G. Standing, *Rapid Commun. Mass Spectrom.* **5**, 117 (1991).
121. K. Riahi, G. Bolbach, A. Brunot, F. Breton, M. Spiro, J.-C. Blais, *Rapid Commun. Mass Spectrom.* **8**, 242 (1994).
122. W. Ens, M. Schürenberg, F. Hillenkamp, *45th ASMS Conference on Mass Spectrometry and Allied Topics* 1099 (1997).
123. R. C. Beavis, *Org. Mass Spectrom.* **27**, 864 (1992).
124. A. Vertes, G. Luo, Y. L., C. Y., I. Marginean, *Appl. Phys. A* **79**, 823 (2004).
125. P. Y. Yau, T. W. D. Chan, P. G. Cullis, A. W. Colburn, P. J. Derrick, *Chem. Phys. Lett.* **202**, 93 (1993).
126. T. W. Heise, E. S. Yeung, *Anal. Chim. Acta* **199**, 377 (1995).
127. D. Feldhaus, C. Menzel, S. Berkenkamp, F. Hillenkamp, *J. Mass Spectrom.* **35**, 1320 (2000).
128. F. Yassin, D. S. Marynick, *J. Mol. Struct.* **629**, 223 (2003).
129. F. H. Yassin, D. S. Marynick, *Mol. Phys.* **103**, 183 (2005).
130. S. Bourcier, S. Bouchonnet, Y. Hoppilliard, *Int. J. Mass Spectrom.* **210/211**, 59 (2001).
131. S. Bourcier, Y. Hoppilliard, *Int. J. Mass Spectrom.* **217**, 231 (2002).
132. Q. Lin, R. Knochenmuss, *Rapid Comm. Mass Spectrom.* **15**, 1422 (2001).
133. G. Kinsel, R. Knochenmuss, P. Setz, C. M. Land, S.-K. Goh, E. F. Archibong, J. H. Hardesty, D. Marynik, *J. Mass Spectrom.* **37**, 1131 (2002).
134. G. R. Kinsel, Q. Zhao, J. Narayanasamy, F. Yassin, H. V. Rasika Dias, B. Niesner, K. Prater, C. St. Marie, L. Ly, D. Marynik, *J. Phys. Chem. A* **108**, 3153 (2004).
135. C. M. Land, G. R. Kinsel, *J. Am. Soc. Mass Spectrom.* **9**, 1060 (1998).
136. C. M. Land, G. R. Kinsel, *J. Am. Soc. Mass Spectrom.* **12**, 726 (2001).
137. F. H. Yassin, D. S. Marynick, *J. Phys. Chem. A* **110**, 3820 (2006).
138. J. F. Ireland, P. A. H. Wyatt, *Adv. Phys. Org. Chem.* **12**, 131 (1976).

139. M. E. Gimon, L. M. Preston, T. Solouki, M. A. White, D. H. Russell, *Org. Mass Spectrom.* **27**, 827 (1992).
140. B. Spengler, R. Kaufmann, *Analisis* **20**, 91 (1992).
141. M. P. Chiarelli, A. G. Sharkey, D. M. Hercules, *Anal. Chem.* **65**, 307 (1993).
142. J. Krause, M. Stoeckli, U. P. Schlunegger, *Rapid Commun. Mass Spectrom.* **10**, 1927 (1996).
143. H. Yong, *Int. J. Mass Spectrom. Ion Proc.* **175**, 187 (1998).
144. H.-C. Lüdemann, F. Hillenkamp, R. Redmond, *J. Phys. Chem. A* **104**, 3884 (2000).
145. S. Niu, W. Zhang, B. T. Chait, *J. Am. Soc. Mass Spectrom.* **9**, 1 (1998).
146. Barthel; J.; Neuder; R.; Schröder; P. *Chemistry Data Series, DCHEMA*; Frankfurt, 1994;
147. K. Breuker, R. Knochenmuss, J. Zhang, A. Stortelder, R. Zenobi, *Int. J. Mass Spectrom.* **226**, 211 (2003).
148. R. Cramer, R. F. Haglund Jr., F. Hillenkamp, *Int. J. Mass Spectrom. Ion Proc.* **169/170**, 51 (1997).
149. M. A. Baldwin, V. L. Talroze, A. L. Burlingame, I. O. Leipunsky, *50th ASMS conference on mass spectrometry and allied topics* (2002).
150. V. L. Talroze, R. L. Jacob, A. L. Burlingame, M. A. Baldwin, *48th ASMS conference on mass spectrometry and allied topics* (2000).
151. V. L. Talroze, R. L. Jacob, A. L. Burlingame, I. O. Leipunsky, M. A. Baldwin, *49th ASMS conference on mass spectrometry and allied topics* (2001).
152. V. L. Talroze, R. L. Jacob, A. L. Burlingame, M. A. Baldwin, *Adv. Mass Spectrom.* **15**, 481 (2001).
153. V. L. Talroze, I. O. Leipunsky, A. L. Burlingame, M. A. Baldwin, *51st ASMS conference on mass spectrometry and allied topics* (2003).
154. V. L. Talroze, I. O. Leipunsky, A. L. Burlingame, M. A. Baldwin, *52nd ASMS conference on mass spectrometry and allied topics* (2004).
155. M. V. Kosevich, V. S. Shelkovsky, O. A. Boryak, V. V. Orlov, *Rapid Comm. Mass Spectrom.* **17**, 1781 (2003).
156. M. L. Vestal, *Mass Spectrom. Rev.* **2**, 447 (1983).
157. V. L. Talroze, M. L. Person, R. M. Whittal, F. C. Walls, A. L. Burlingame, M. A. Baldwin, *Rapid Comm. Mass Spectrom.* **13**, 21914 (1999).
158. R. Knochenmuss, A. Stortelder, K. Breuker, R. Zenobi, *J. Mass Spectrom.* **35**, 1237 (2000).
159. G. R. Kinsel, D. Yao, F. H. Yassin, D. S. Marynick, *Eur. J. Mass Spectrom.* **submitted**, (2006).
160. M. Mormann, S. M. Bashir, P. J. Derrick, D. Kuck, *J. Am. Soc. Mass Spectrom.* **11**, 544 (2000).
161. T. J. D. Jørgensen, G. Bojesen, H. Rahbek-Nielsen, *Eur. Mass Spectrom.* **4**, 39 (1998).
162. T. J. D. Jørgensen, T. Vulpius, G. Bojesen, *13th International Mass Spectrometry Conference* 175 (1994).
163. R. D. Burton, C. H. Watson, J. R. Eyler, G. L. Lang, D. H. Powell, M. Y. Avery, *Rapid Commun. Mass Spectrom.* **11**, 443 (1997).
164. R. J. J. M. Steenvoorden, K. Breuker, R. Zenobi, *Eur. Mass Spectrom.* **3**, 339 (1997).
165. K. Breuker, R. Knochenmuss, R. Zenobi, *Int. J. Mass Spectrom.* **184**, 25 (1999).

166. K. Breuker, R. Knochenmuss, R. Zenobi, *J. Am. Soc. Mass Spectrom.* **10**, 1111 (1999).
167. S. P. Mizra, N. P. Raju, M. Vairamani, *J. Am. Soc. Mass Spectrom.* **15**, 431 (2004).
168. J. Zhang, E. Dyachova, T.-K. Ha, R. Knochenmuss, R. Zenobi, *J. Phys. Chem. A* **107**, 6891 (2003).
169. J. Zhang, T.-K. Ha, R. Knochenmuss, R. Zenobi, *J. Phys. Chem. A* **106**, 6610 (2002).
170. J. Zhang, R. Knochenmuss, E. Stevenson, R. Zenobi, *J. Mass Spectrom.* **213**, 237 (2002).
171. C. T. J. Scott, C. Kosmidis, W. J. Jia, K. W. D. Ledingham, R. P. Singhal, *Rapid Commun. Mass Spectrom.* **8**, 829 (1994).
172. N. L. Asfandiarov, S. A. Pshenichnyuk, A. I. Forkin, V. G. Lukin, V. S. Fal'ko, *Rapid Commun. Mass Spectrom.* **16**, 1760 (2002).
173. J. Sunner, *Org. Mass Spectrom.* **28**, 805 (1993).
174. Harrison; A. G. *Chemical Ionization Mass Spectrometry*; CRC Press: Boca Raton, 1992;
175. T.-W. D. Chan, A. W. Colburn, P. J. Derrick, *Org. Mass Spectrom.* **27**, 53 (1992).
176. T.-W. D. Chan, A. W. Colburn, P. J. Derrick, *Org. Mass Spectrom.* **26**, 342 (1991).
177. R. Knochenmuss, F. Dubois, M. J. Dale, R. Zenobi, *Rapid Commun. Mass Spectrom.* **10**, 871 (1996).
178. R. Knochenmuss, V. Karbach, U. Wiesli, K. Breuker, R. Zenobi, *Rapid Commun. Mass Spectrom.* **12**, 529 (1998).
179. G. McCombie, R. Knochenmuss, *Anal. Chem.* **76**, 4990 (2005).
180. Y. Dai, R. M. Whittal, L. Li, *Anal. Chem.* **68**, 2494 (1996).
181. V. Horneffer, A. Forsmann, K. Strupat, F. Hillenkamp, U. Kubitscheck, *Anal. Chem.* **73**, 1016 (2001).
182. R. W. Garden, J. V. Sweedler, *Anal. Chem.* **72**, 30 (2000).
183. S. L. Luxembourg, L. A. McDonnell, M. C. Duursma, X. Guo, R. M. A. Heeren, *Anal. Chem.* **75**, 2333 (2003).
184. A. G. Harrison, *Mass Spectrom. Rev.* **16**, 201 (1997).
185. M. L. Valreo, E. Giralt, D. Andreu, *Lett. Peptide Sci.* **6**, 109 (1999).
186. S. Baumgart, Y. Lindner, R. Kuehne, A. Oberem, H. Wenschuh, E. Krause, *Rapid Comm. Mass Spectrom.* **18**, 863 (2004).
187. H. Wenschuh, P. Halada, S. Lamer, P. Jungblut, E. Krause, *Rapid Commun. Mass Spectrom.* **12**, 115 (1998).
188. T. Nishikaze, M. Takayama, *Rapid Comm. Mass Spectrom.* **20**, 376 (2006).
189. W. I. Burkitt, A. E. Giannakopoulos, F. Sideridou, S. Bashir, P. J. Derrick, *Aust. J. Chem.* **56**, 369 (2003).
190. S. R. Carr, C. J. Cassidy, *J. Am. Soc. Mass Spectrom.* **7**, 1203 (1996).
191. S. R. Carr, C. J. Cassidy, *J. Mass Spectrom.* **32**, 959 (1997).
192. Z. Olumee, A. Vertes, *J. Phys. Chem. B* **102**, 6118 (1998).
193. C.-W. Chou, P. Williams, P. A. Limbach, *Int. J. Mass Spectrom.* **193**, 15 (1999).
194. Freiser; B. S. *Organometallic Ion Chemistry*; Kluwer: Dordrecht, 1996; pp 238.
195. J. S. Klassen, S. G. Anderson, A. T. Blades, P. Kebarle, *J. Phys. Chem.* **100**, 14218 (1996).
196. S. Hoyau, K. Norrman, T. B. McMahon, G. Ohanessian, *J. Am. Chem. Soc.* **121**, 8864 (1999).

197. S. Hoyau, G. Ohanessian, *Chem. Eur. J.* **8**, 1561 (1998).
198. J. Zhang, R. Zenobi, *J. Mass Spectrom.* **39**, 808 (2004).
199. H. Rashidezadeh, B. Guo, *J. Am. Soc. Mass Spectrom.* **9**, 724 (1998).
200. B. H. Wang, K. Dreisewerd, U. Bahr, M. Karas, F. Hillenkamp, *J. Am. Soc. Mass Spectrom.* **4**, 393 (1993).
201. W. J. Erb, K. G. Owens, S. D. Hanton, *52nd ASMS Conference on Mass Spectrometry and Allied Topics* (2004).
202. S. D. Hanton, K. G. Owens, C. Chavez-Eng, A.-M. Hoberg, P. J. Derrick, *Eur. J. Mass Spectrom.* **11**, 23 (2005).
203. S. Trimpin, A. Rouhanipour, R. Az, H. J. Rader, K. Mullen, *Rapid Comm. Mass Spectrom.* **15**, 1364 (2001).
204. S. D. Hanton, D. M. Parees, *J. Am. Soc. Mass Spectrom.* **16**, 90 (2004).
205. A. J. Hoteling, K. G. Owens, *53rd ASMS conference on mass spectrometry and allied topics* (2005).
206. S. D. Hanton, K. G. Owens, W. Blair, I. Z. Hyder, J. R. Stets, C. M. Guttman, A. Giuseppi, *J. Amer. Soc. Mass Spectrom.* **15**, 168 (2004).
207. P. Lecchi, M. Olson, F. L. Brancia, *J. Am. Soc. Mass Spectrom.* **16**, 1269 (2005).
208. P. Juhasz, C. E. Costello, *Rapid Commun. Mass Spectrom.* **7**, 343 (1993).
209. T. D. McCarley, R. L. McCarley, P. A. Limbach, *Anal. Chem.* **70**, 4376 (1998).
210. S. F. Macha, T. D. McCarley, P. A. Limbach, *Anal. Chim. Acta* **397**, 235 (1999).
211. A. Streletskii, I. N. Ioffe, S. G. Kotsiris, M. P. Barrow, T. Drewello, S. H. Strauss, O. G. Boltalina, *J. Phys. Chem. A* **109**, 714 (2005).
212. R. Lidgard, M. W. Duncan, *Rapid Commun. Mass Spectrom.* **9**, 128 (1995).
213. L. Ulmer, J. Mattay, H. G. Torres-Garcia, H. Luftmann, *Eur. J. Mass Spectrom.* **6**, 49 (2000).
214. T. Brown, N. L. Clipston, N. Simjee, H. Luftmann, H. Hungerbuhler, T. Drewello, *Int. J. Mass Spectrom.* **210/211**, 249 (2001).
215. R. A. Marcus, *J. Chem. Phys.* **24**, 966 (1956).
216. R. Knochenmuss, E. Lehmann, R. Zenobi, *Eur. Mass Spectrom.* **4**, 421 (1998).
217. T. Yalcin, D. C. Schriemer, L. Li, *J. Am. Soc. Mass Spectrom.* **8**, 1220 (1997).
218. J. Zhang, V. Frankevich, R. Knochenmuss, S. D. Friess, R. Zenobi, *J. Am. Soc. Mass Spectrom.* **14**, 42 (2002).
219. R. W. Nelson, T. W. Hutchens, *Rapid Commun. Mass Spectrom.* **6**, 4 (1992).
220. A. S. Woods, J. C. Buchsbaum, T. A. Worall, J. M. Berg, R. J. Cotter, *Anal. Chem.* **67**, 4462 (1995).
221. D. R. Lide, (1992).
222. E. R. Williams, *J. Mass Spectrom.* **31**, 831 (1996).
223. X. Zhang, C. J. Cassady, *J. Am. Soc. Mass Spectrom.* **7**, 1211 (1996).
224. G. A. Pallante, C. J. Cassady, *Int. J. Mass Spectrom.* **12075**, 1 (2002).
225. D. S. Gross, E. R. Williams, *J. Amer. Chem. Soc.* **118**, 202 (1996).
226. R. Knochenmuss, *Anal. Chem.* **75**, 2199 (2003).
227. N. Agmon, *Int. J. Chem. Kin.* **13**, 333 (1981).
228. N. Agmon, R. D. Levine, *Israel J. Chem.* **19**, 330 (1980).
229. E. Moskovets, A. Vertes, *J. Phys. Chem. B* **106**, 3301 (2002).
230. R. C. Beavis, J. N. Bridson, *J. Phys. D - Appl. Phys.* **26**, 442 (1993).
231. M. Sadeghi, A. Vertes, *Appl. Surf. Sci.* **127/129**, 226 (1998).
232. F. Xiang, R. C. Beavis, *Org. Mass Spectrom.* **28**, 1424 (1993).
233. G. McCombie, R. Knochenmuss, *J. Am. Soc. Mass Spectrom.* **17**, 737 (2006).

234. V. Frankevich, J. Zhang, M. Dashtiev, R. Zenobi, *Rapid Comm. Mass Spectrom.* **17**, 2343 (2003).
235. V. Frankevich, J. Zhang, S. D. Friess, M. Dashtiev, R. Zenobi, *Anal. Chem.* **75**, 6063 (2003).
236. L. Lyons, **Physics and Chemistry of the Organic Solid State** **1**, 745 (1963).
237. K. Seki, N. Hayashi, H. Oji, E. Ito, Y. Ouchi, *Thin Solid Films* **393**, 298 (2001).
238. M. Dashtiev, V. Frankevich, R. Zenobi, *J. Phys. Chem. A* **110**, 926 (2006).
239. R. Knochenmuss, G. McCombie, M. Faderl, *J. Phys. Chem. A* **submitted**, (2006).
240. A. F. Altelaar, I. Klinkert, K. Jalink, R. P. J. deLange, R. A. H. Adan, R. M. A. Heeren, S. R. Piersma, *Anal. Chem.* **78**, 734 (2006).
241. J. A. McLean, K. A. Stumpo, D. H. Russell, *J. Am. Chem. Soc.* **127**, 5304 (2004).
242. I. A. Kaltashov, D. Fabris, C. Fenselau, *J. Phys. Chem.* **99**, 10046 (1995).
243. P. D. Schnier, D. S. Gross, E. R. Williams, *J. Am. Chem. Soc.* **117**, 6747 (1995).
244. G. S. Gorman, J. P. Speir, C. A. Turner, I. J. Amster, *J. Am. Chem. Soc.* **114**, 3986 (1992).
245. S. G. Lias, H. M. Rosenstock, K. Draxl, B. W. Steiner, J. T. Herron, J. L. Holmes, R. D. Levin, J. F. Liebman, S. A. Kafafi, **NIST Standard Reference Database No. 69** (1998).

Figures

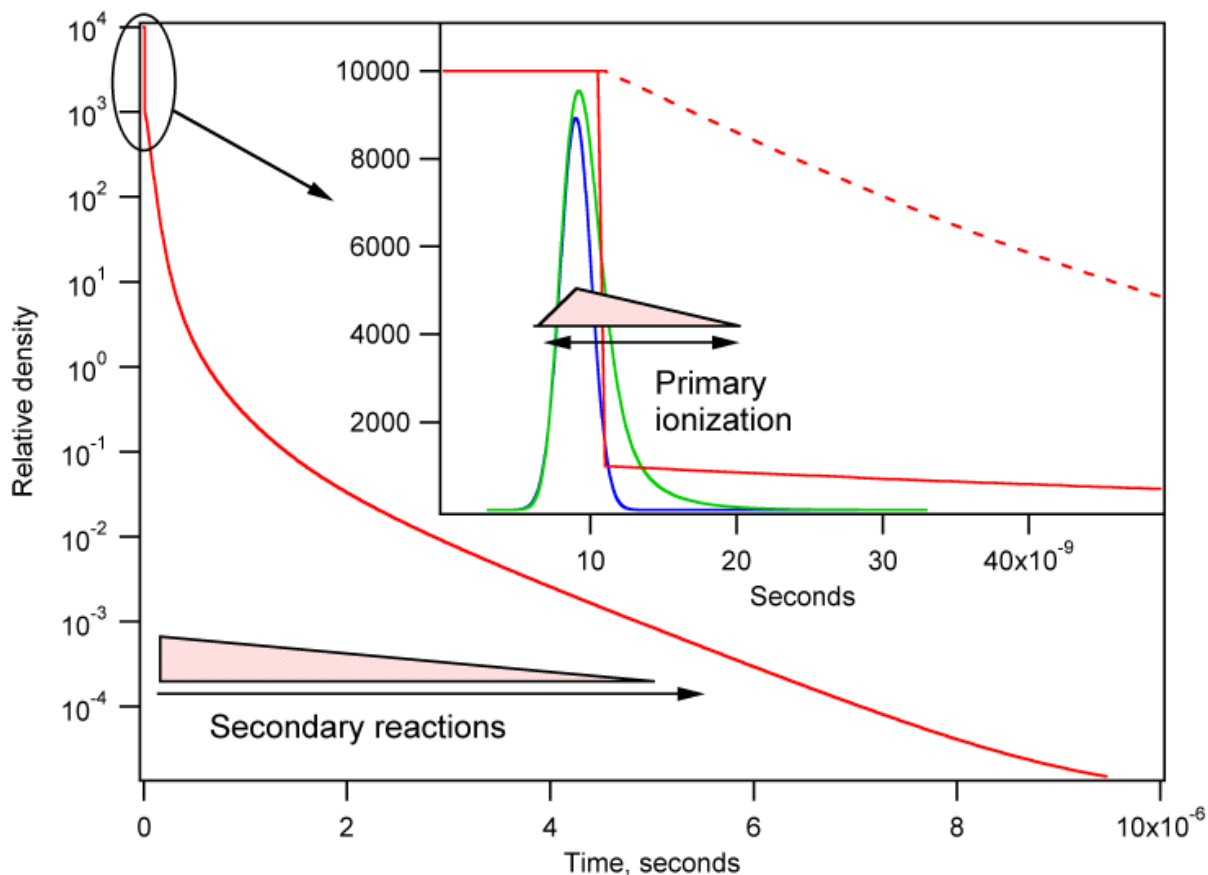


Figure 1. The origin of the 2-step model: expansion of the MALDI plume compared to the laser pulse and excited state decay. Density is plotted vs. time for a plume expanding as an adiabatic free jet. A density of 1 is approximately that of a gas at 1 atm. The expansion stops when the gas reaches the environmental background pressure, which may vary in practice from 1 atm. to high vacuum. The inset shows the early behavior, along with a 3 ns N_2 laser pulse (blue) and the typical lifetime of matrix excited states (green). Only during the time when energy and material densities are high can significant ionization occur. The solid line represents the density if the sample vaporizes smoothly. The dashed line represents an explosive phase change for which a well-defined solid-gas boundary may not exist at short times.

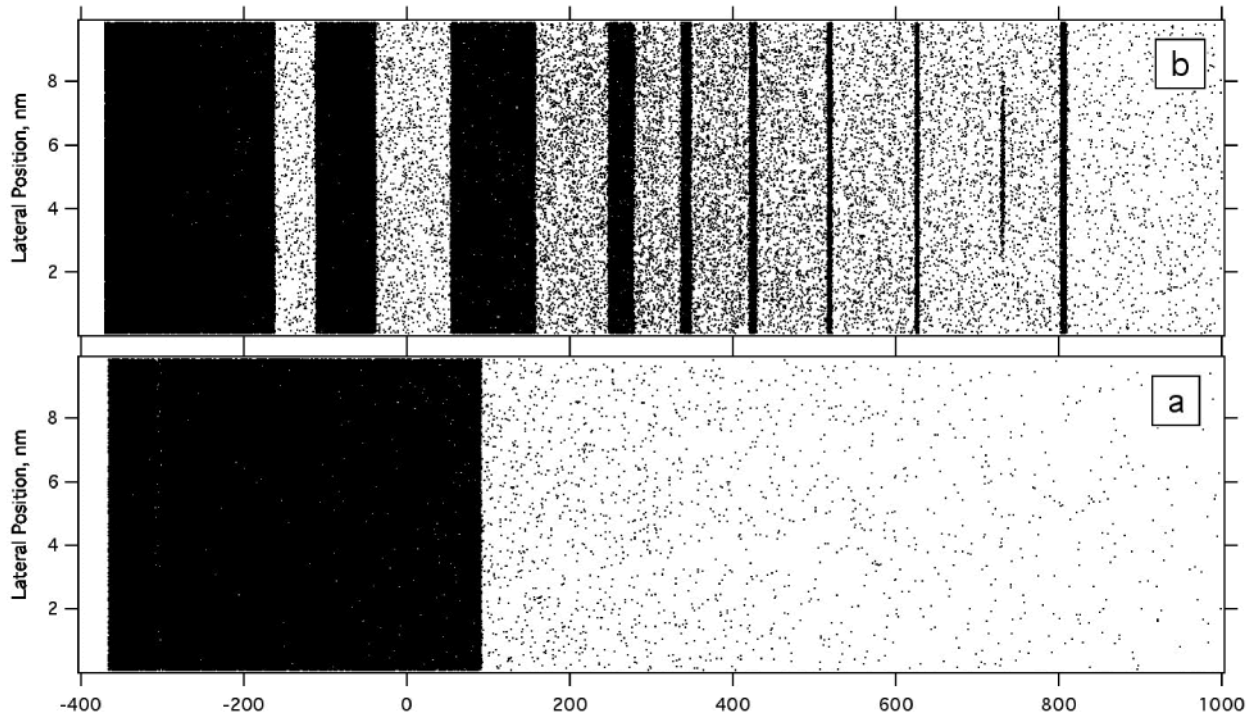


Figure 2. Snapshots of simulated MALDI events in the desorption (a) and ablation (b) regimes. Both generate ions, but the latter also generates condensed fragments of the original solid (clusters). These cool in the entraining gas and do not evaporate in the simulation. Adapted from ref 59.

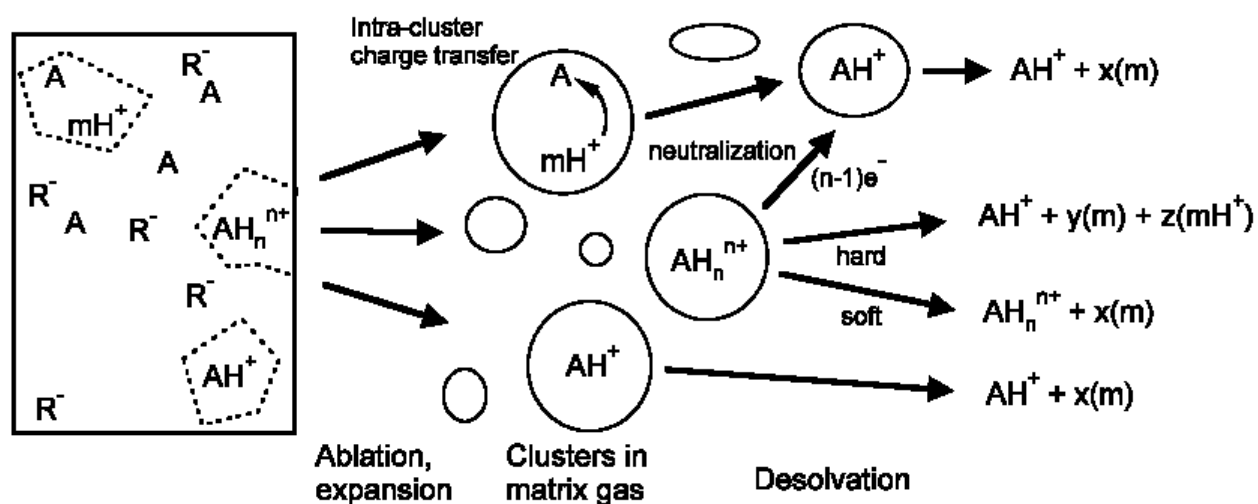


Figure 3. Sketch of the major processes proposed in cluster models of MALDI ionization. m=matrix, A=analyte, R⁻=generic counterion. Preformed ions, separated in the preparation solution, are contained in clusters ablated from the initial solid material. Some clusters contain a net excess of positive charge, others net negative (not shown). If analyte is already charged, here by protonation, cluster evaporation may free the ion. In other clusters charge may need to migrate from its initial location, e.g. on matrix, to the more favorable location on analyte (secondary reaction). For multiply charged analytes, hard and soft desolvation processes may lead to different free ions. Neutralization by electrons or counterions takes place to some degree, but is not complete.

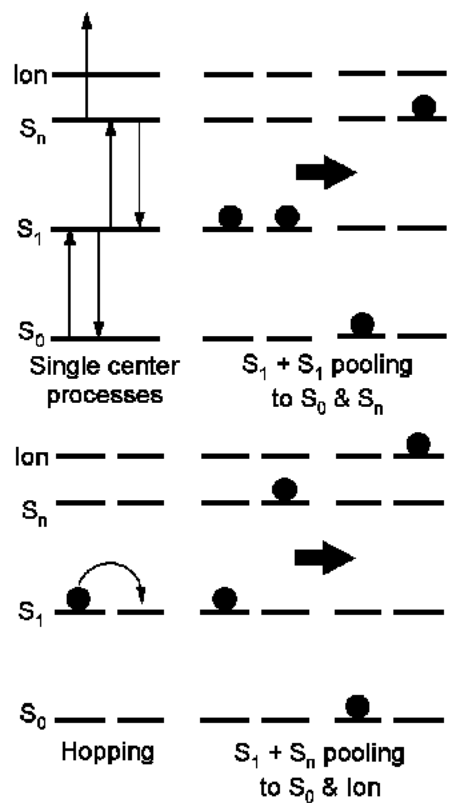


Figure 4. Unimolecular and biomolecular matrix processes included in the MALDI ionization model of refs. 60, 226. Pooling reactions of matrix excited states are key steps in energy concentration and ionization.

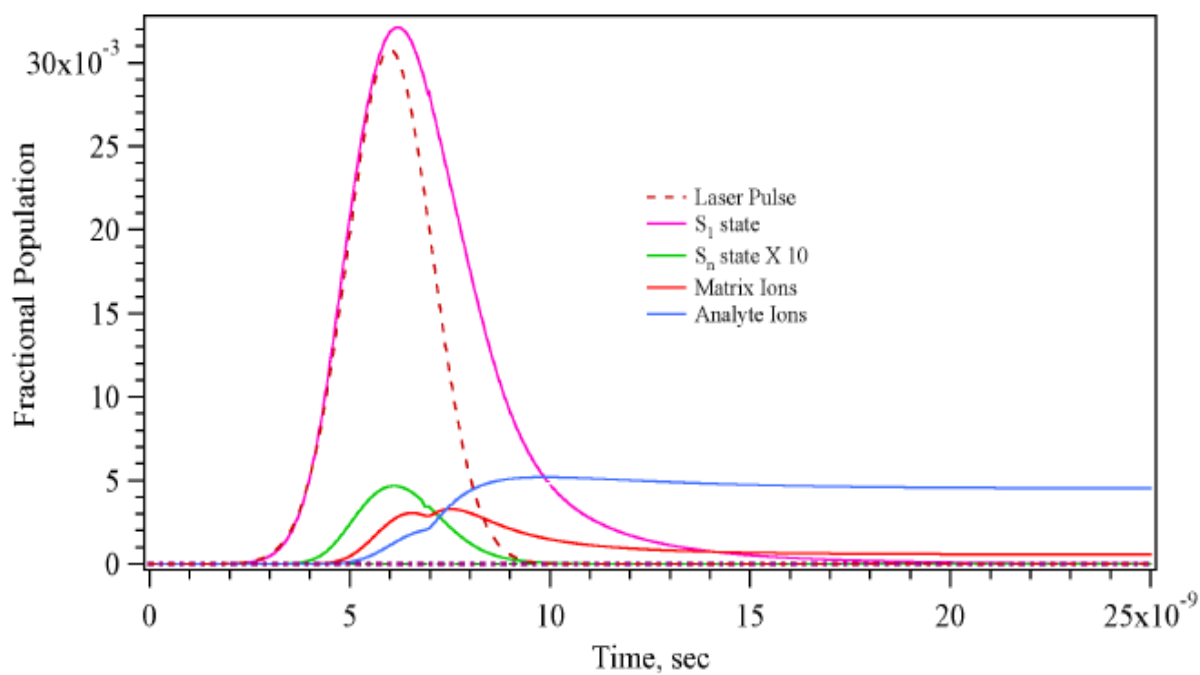


Figure 5. Example of the time-dependent evolution of a MALDI sample in the photoionization/pooling model. Pooling of abundant S_1 excitations leads to higher excited S_n matrix molecules. Pooling of S_1 and S_n leads to matrix ions (primary ionization). These react with analyte neutrals to yield analyte ions (secondary ionization), depleting the matrix ion signal.

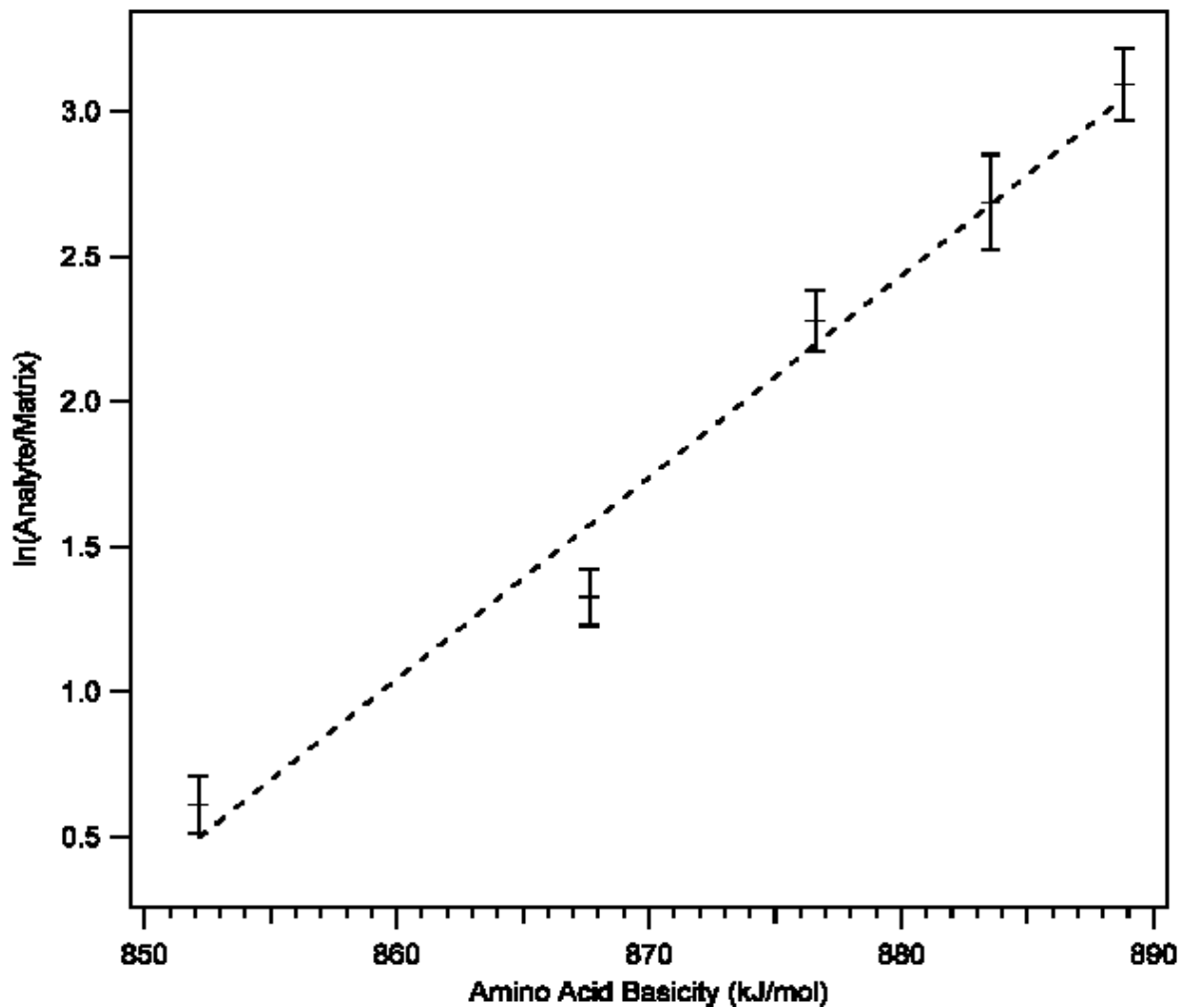


Figure 6: Equilibrium plot for the MALDI ion signals of the amino acids G, A, V, I, and F in the matrix CHCA, versus the amino acid basicity, and hence the matrix-analyte proton transfer reaction free energy. The linearity indicates that near equilibrium is reached in the plume for charge transfer reactions of matrix and analyte. Adapted from ref. 159.

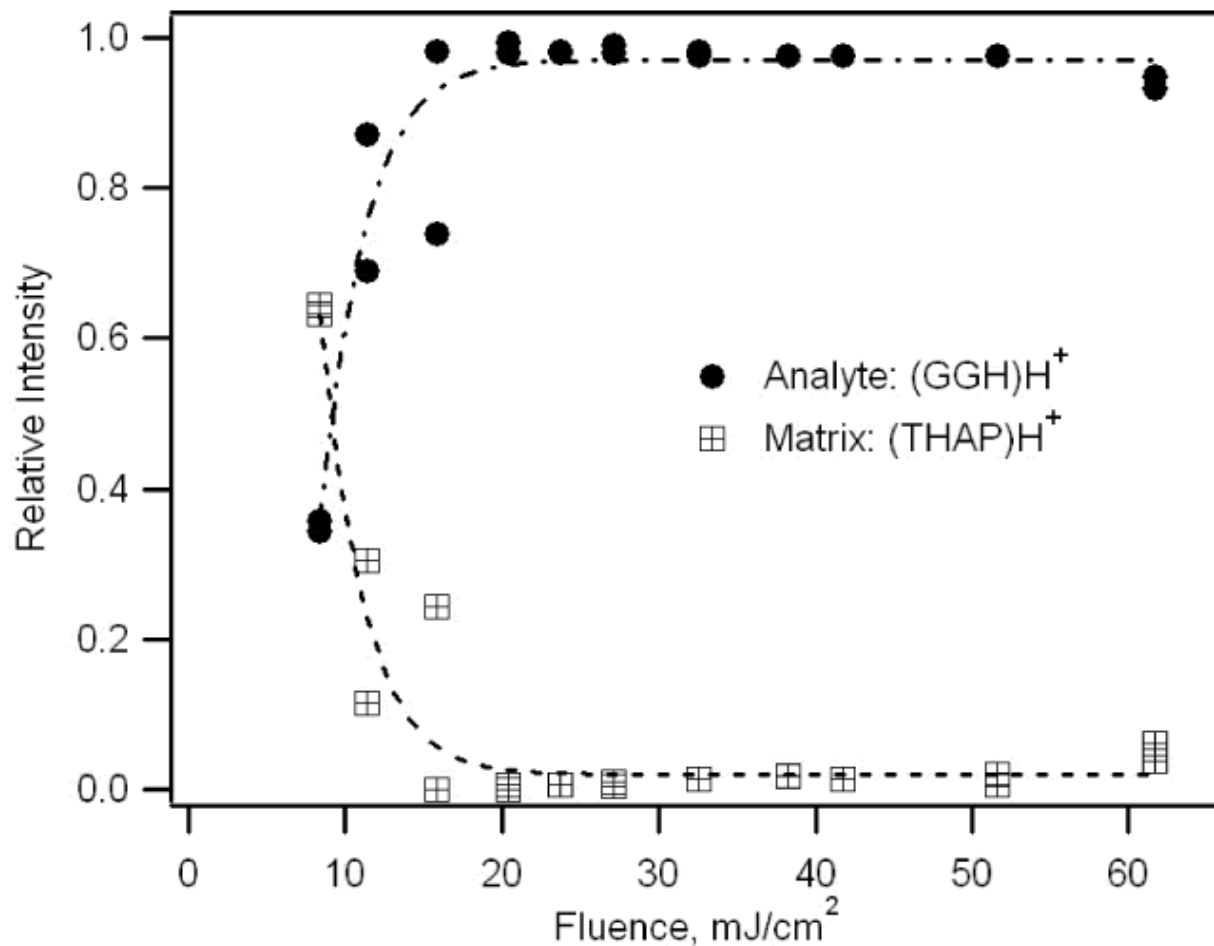


Figure 7. Normalized intensities of positive MALDI ions obtained from a sample of glycyl–glycyl–histidine in 2,4,6-trihydroxyacetophenone matrix (1:1 molar ratio) vs. laser fluence. Matrix suppression is essentially complete at most fluences, but not near threshold. This is a consequence of incomplete secondary reactions of primary matrix ions with neutral analytes. Adapted from ref. 147.

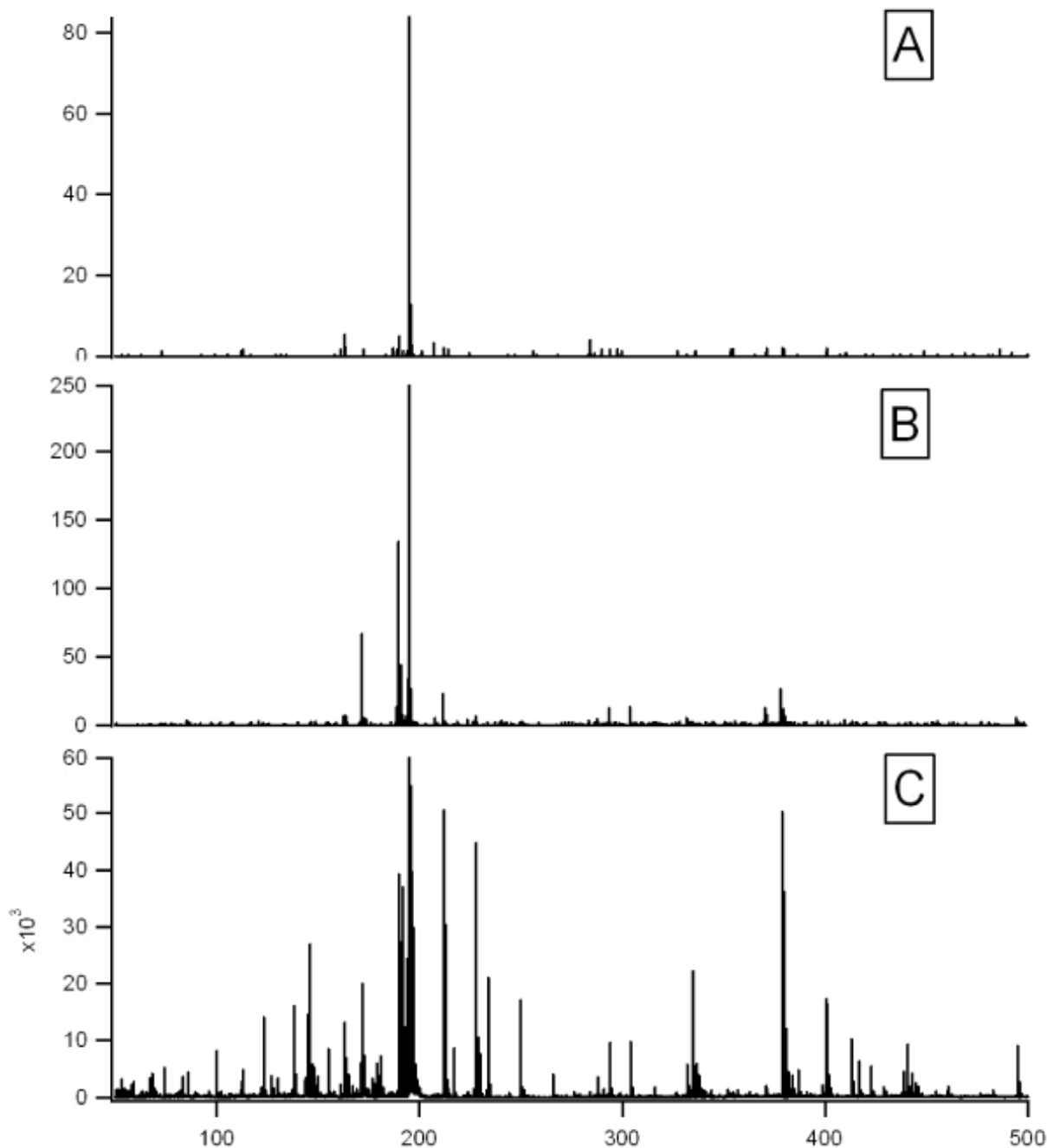


Figure 8. MALDI-TOF mass spectra of caffeine, in CHCA matrix. When more analyte is present than primary ions, suppression occurs as a consequence of secondary reactions. This ratio is affected by both the analyte concentration and the laser intensity. Matrix suppression is nearly complete in spectrum A, where the matrix/analyte ratio is low ($M/A=3$). At higher ratio, $M/A=27$, more matrix signals appear, as seen in spectrum B. In panel C, the matrix:analyte mole ratio was again 3 but more matrix signals appear as a result of much higher laser pulse energy. Adapted from ref. 179.

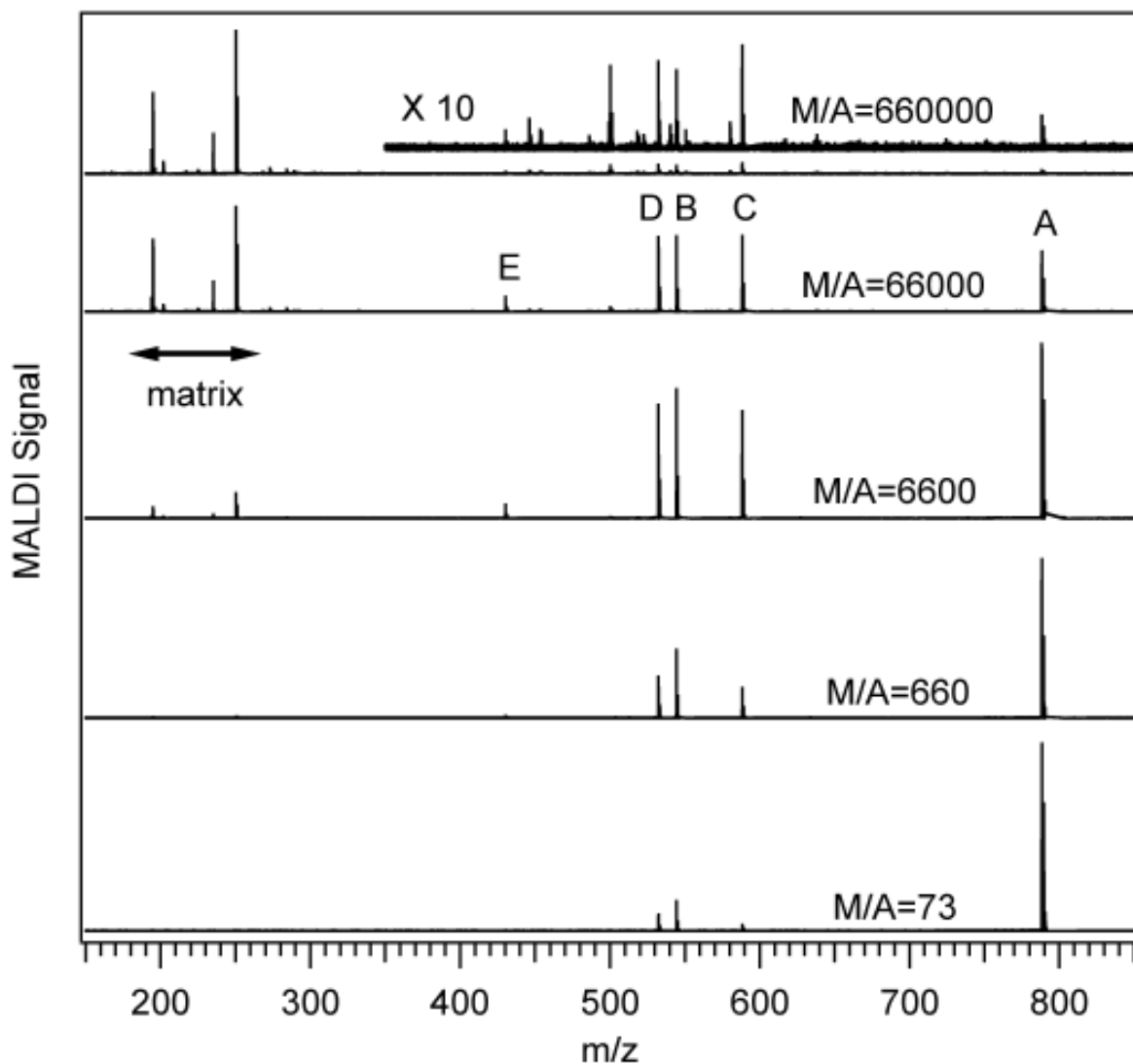


Figure 9. Positive mode MALDI spectra vs. matrix/analyte mole ratio (DCTB matrix) for an equimolar five-component mixture. A= M-Tdata, ionization potential (IP)=6.04 eV (CAS number: 124729-98-2), B= TTb, IP=6.28 eV (76185-65-4), C=NPB, IP=6.45 eV (123847-85-8), D=rubrene, IP=6.50 eV (104751-29-9), E=D2NA, IP=7.06 eV (122648-99-1). The molar mixing ratios of matrix to analyte are indicated for each spectrum. These analytes are observed exclusively as radical cations, and exhibit matrix and analyte suppression effects analogous to those known from proton or cation transfer secondary reactions. Low ionization potential (IP) analytes suppress high IP analytes and matrix. Adapted from ref. 116.

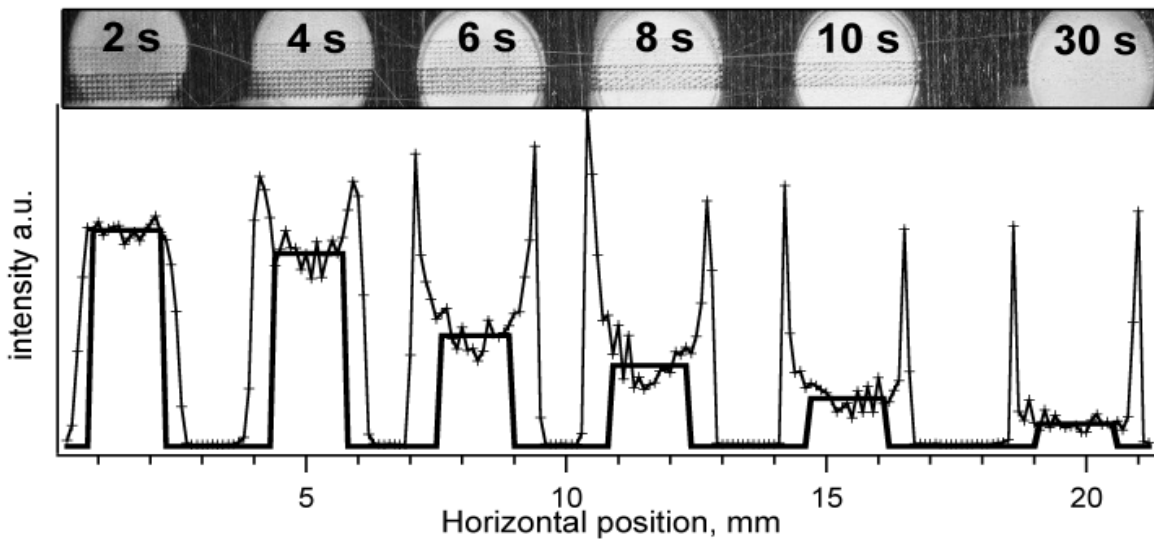


Figure 10. Electro sprayed MALDI spots of reserpine and substance P in DHB matrix, on stainless steel. Spray times are shown on the optical image of the spots after MALDI measurement. The thickness was estimated to be 100 nm per second of spray time, and the distance between laser craters is 0.1 mm. The traces in the lower panel show the substance P signals summed over five vertical columns. The traces with symbols are the measured values. In the regions where it is not zero, the solid line is the average value of the most uniform central region of each spot. The significant enhancement of signal for the thinnest spots and thin edges is apparent. Adapted from ref. 233.

Table 1. Selected thermodynamic quantities relevant to MALDI primary and secondary ionization.

Substance	number of prior protons	PA (kJ/mol)	GB (kJ/mol)	Reference
Gramicidin S	n=1		916.7 ± 11.7	225
	n=0		>1018.0	225
Bradykinin	n=1		968.2	242
	n=0		>1025.1	242
Leucine-enkephalin	n=0		967.8 ± 2.1	242
Cytochrome C	n=5		735	243
	n=4		722	243
	n=3		673	243
Gly		885 ± 13		244
		859.9		863 244
His		955 ± 9		244
		969.2		937 184
Arg		>1016.		244
		1025		992 184
		1037 (H-bonded)		184
Gly-Gly-Pro			908	184
Gly-Pro-Gly			908	184
Pro-Gly-Gly			916	184
Gly-Gly-His			948-959	184
Gly-His-Gly			943-946	184
His-Gly-Gly			948-953	184
Gly-Gly-Arg			1015	184
Gly-Lys-Lys-Gly-Gly			995	184
Gly-Lys-Gly-Lys-Gly			998	184
Lys-Gly-Gly-Gly-Lys			1015	184
Matrix	PA (kJ/mol)	GB (kJ/mol)	GB((M-H)-) (kJ/mol)	Reference
a-cyano-4-hydroxycinnamic acid (4HCCA)	841			161
	765.7 ± 8.4			163
	933 ± 9	900.5 ± 8.5		164
	841.5			167
	854 ± 14	822.5 ± 15.5		164
4HCCA-H ₂ O	854 ± 14	822.5 ± 15.5		164
4HCCA-CO ₂	894.5 ± 13.5	860.5 ± 11.5		164
Dihydroxybenzoic acid isomers:				
	2,5-DHB	855 ± 8	822 ± 8	160
		853.5 ± 16.7		163
		854 ± 14	822.5 ± 15.5	164
		850.4	819.8	129
	855.8		167	
			1329	165
				129
2,6-DHB	864 ± 6	830 ± 6		160
	855.2	823.6		129

			1284	128
Ferulic acid	879			161
	765.7 ± 8.4			163
Sinapinic acid (SA)	887			161
	894.5 ± 13.5	860.5 ± 11.5		164
	875.9			167
SA-H2O	933 ± 9	900.5 ± 8.5		164
SA-H2O-HOCH3	854 ± 14	822.5 ± 15.5		164
Nicotinic acid	907			161
	899.6 ± 16.7			163
3-Hydroxypicolinic acid (3HPA)	896			161
	898.5			167
			1365	165
2-(4-Hydroxyphenylazo)benzoic acid (HABA)	943			161
	765.7 ± 8.4			163
	950			167
trans-3-Indoleacrylic acid (IAA)	899.6 ± 16.7			163
	893.9			167
Dithranol (1,8-dihydroxyanthrone)	874.5 ± 8.4			163
	885.5			167
3,5-Dimethoxyhydroxycinnamic acid	853.5 ± 16.7			163
2,4,6-Trihydroxyacetophenone (THAP)	882			165
	893			167
			1324	165
Matrix	IP(eV)			Reference
2,5 DHB	8.054			115
	8.14			129
	8.19			116
	7.86			131
2,6 DHB	8.3			129
HABA	8.32			116
IAA	7.75			116
Dithranol (1,8-dihydroxyanthrone)	8.17			116
4HCCA	8.5			116
SA	8.67			116
THAP	8.44			116
Nicotinic acid	9.38			245
	9.63			116
	9.21			131
3HPA	8.95			131